Bulletin of the Seismological Society of America, 90, 6B, pp. S1–S31, December 2000

Accounting for Site Effects in Probabilistic Seismic Hazard Analyses of Southern California: Overview of the SCEC Phase III Report

by Edward H. Field* and the SCEC Phase III Working Group†

Abstract This article presents an overview of the Southern California Earthquake Center (SCEC) Phase-III effort to determine the extent to which probabilistic seismic hazard analysis (PSHA) can be improved by accounting for site effects. The contributions made in this endeavor are represented in the various articles that compose this special issue of BSSA.

Given the somewhat arbitrary nature of the site-effect distinction, it must be carefully defined in any given context. With respect to PSHA, we define the site effect as the response, relative to an attenuation relationship, averaged over all damaging earthquakes in the region. A diligent effort has been made to identify any attributes that predispose a site to greater or lower levels of shaking. The most detailed maps of Quaternary geology are not found to be helpful; either they are overly detailed in terms of distinguishing different amplification factors or present southern California strong-motion observations are inadequate to reveal their superiority. A map based on the average shear-wave velocity in the upper 30 m, however, is found to delineate significantly different amplification factors. A correlation of amplification with basin depth is also found to be significant, implying up to a factor of two difference between the shallowest and deepest parts of the Los Angeles basin. In fact, for peak acceleration the basin-depth correction is more influential than the 30-m shear-wave velocity. Questions remain, however, as to whether basin depth is a proxy for some other site attribute.

In spite of these significant and important site effects, the standard deviation of an attenuation relationship (the prediction error) is not significantly reduced by making such corrections. That is, given the influence of basin-edge-induced waves, subsurface focusing, and scattering in general, any model that attempts to predict ground motion with only a few parameters will have a substantial intrinsic variability. Our best hope for reducing such uncertainties is via waveform modeling based on first principals of physics.

Finally, questions remain with respect to the overall reliability of attenuation relationships at large magnitudes and short distances. Current discrepancies between viable models produce up to a factor of 3 difference among predicted 10% in 50-yr exceedance levels, part of which results from the uncertain influence of sediment nonlinearity.

Introduction

There are generally two end-member approaches for estimating earthquake ground motion. One is probabilistic seismic hazard analysis, (PSHA) (Cornell, 1968; Reiter, 1990), which accounts for all potentially damaging earthquakes in a region, but where ground motion is represented with a relatively simple parameter (such as peak acceleration or a response spectrum ordinate). The other approach is waveform modeling of a complete synthetic seismogram (e.g., Spudich and Hartzell, 1985; Aki *et al.,* 1995), which can be applied in dynamic analyses to account for effects such as shaking duration and nonlinear structural response. The two approaches are actually complementary, where the

*Present Address: U.S. Geological Survey, 525 South Wilson Ave, Pasadena, California, 91106

†(alphabetical order) John G. Anderson, Thomas L. Henyey, David D. Jackson, William B. Joyner, Yajie Lee, Harold Magistrale, Bernard Minster, Kim B. Olsen, Mark D. Petersen, Jamison H. Steidl, Lisa A. Wald, and Chris J. Wills

composite hazard given by PSHA can be disaggregated to find the most menacing earthquake scenarios at a particular site, and then synthetic seismograms can be generated for those events. In fact, we can envision the day when a PSHA hazard map is on-line, and by clicking on a particular location, a suite of representative synthetic seismograms is provided (Spudich, 1997).

Because both waveform modeling and dynamic analyses are in a relatively early stage of development, their application is generally reserved for critical facilities. Although PSHA is more deeply rooted in engineering practice, a fact reflected in current building codes (e.g., BSSC, 1995, 1998), important questions remain with respect to representing both earthquake sources (e.g., Field *et al.,* 1999; Petersen *et al.,* 2000) and wave-propagation effects (e.g., Senior Seismic Hazard Analysis Committee [SSHAC], 1997). Finally, it should be noted that PSHA and waveform modeling are not completely independent, as waveform modeling has been used to develop attenuation relationships for low-seismicity regions (e.g., Toro *et al.,* 1997), and synthetic seismograms are often rescaled in practice to be consistent with empirical attenuation relationships (N. Abrahamson, written comm., 1999). Nevertheless, the distinction provides a useful conceptual framework as we seek a more complete representation of seismic hazard.

With funding primarily from the National Science Foundation and the United States Geological Survey (USGS), a consortium of academic, industry, and governmental organizations formed the Southern California Earthquake Center (SCEC) in 1991. The rationale for establishing SCEC was to facilitate an interdisciplinary, system level approach to earthquake hazard analysis. As stated in the original proposal, the specific goal was to do the following:

> integrate research findings from various disciplines in earthquake-related science to develop a prototype probabilistic seismic hazard model (master model) for southern California. In essence, . . . the solid earth dynamics equivalent of global atmospheric and ocean circulation models. . . .

The first milestone toward achieving this goal was the Phase II report (Working Group on California Earthquake Probabilities [WGCEP] 1995), which represented a large-scale effort to integrate seismic, geologic, and geodetic information into a single model of earthquake occurrence for southern California. As is often the case with scientific endeavors of this scale, the report seemed to raise more questions than it answered, particularly in terms of a discrepancy between observed and predicted seismicity rates (see Field *et al.* (1999) for the most recent overview). This problem was inherited by the subsequent generation of official seismic-hazard maps for California (Petersen *et al.,* 1996; Petersen *et al.,* 2000), which remain in use today. A recent working group has already revised earthquake probabilities for northern California (WGCEP, 1999), and a separate effort has been initiated by SCEC and the USGS to improve seismic hazard source models in southern California (*http://www.scec.org/research/RELM*).

The other element needed for PSHA is the ground-motion model. All of the studies mentioned thus far examined hazard for rock-site conditions only. In fact, as discussed subsequently, today's building codes are based on rock-site hazard maps and apply a site correction at a later stage. A more sophisticated and presumably reliable approach would be to apply site corrections within the hazard calculations directly. However, it has not been entirely clear how this should be done, as reflected by the fact that the most comprehensive treatment of PSHA to date (SSHAC, 1997), left the issue to future studies.

To fill this gap, SCEC initiated the Phase III effort in 1994. The goal has been to determine how, and to what extent, site effects can be accounted for in PSHA. The findings of the Phase III working group are presented in the various articles that compose this special issue of the BSSA, with this article providing an overview. The project has evolved dramatically since its inception, with significant contributions being made by several participants not part of the original Phase III working group (Joyner, 2000; Magistrale *et al.,* 2000, Wald and Mori, 2000; Wills *et al.,* 2000).

While we have concentrated on incorporating site effects in PSHA, many of our findings should be useful for waveform modeling as well. In fact, several of the Phase III papers use synthetic seismograms to address PSHA-related questions (Olsen, 2000; Anderson, 2000; Ni *et al.,* 2000). Furthermore, while the SCEC master-model goal was originally articulated in terms of PSHA, considerable resources have been devoted to waveform modeling as well (e.g., Aki *et al.,* 1995). Finally, it should be noted that SCEC does not make official hazard estimates. Rather, it applies an interdisciplinary approach to developing and testing the ingredients for seismic hazard analysis, and then distributes these results to users and government organizations in charge of hazard estimation.

This article is not intended to provide a comprehensive discourse on the physics of site response, nor does it represent a thorough review of the literature. Rather, the level of discussion has been economized with respect to accounting for site effects in PSHA of southern California. Readers interested in less provincial and/or more general reviews are referred to Aki (1988), Aki and Irikura (1991), Bard (1994), and to the proceedings of the Second International Symposium on the Effects of Surface Geology on Seismic Motion (Yokohama, Japan, 2–3 December 1998). Additional discussion and references can also be found in the individual articles that make up this issue.

Although our focus is on southern California, many of our findings should point to potentially useful lines of inquiry in other regions as well. However, there are some important conditions that have not been addressed in this collection of papers, such as the behavior of very soft sediments like San Francisco bay mud, which are much less pervasive in southern California. We have also ignored vertical-component ground motion.

Finally, history has shown that while scientific theories may be fleeting, the longest-lasting legacies of projects of this scope are often the data sets they generate. Therefore, a web page has been established to facilitate data distribution (*http://www.scec.org/research/phase3*). This site also contains several web-based applications that allow users to evaluate and test various attenuation relationships with different input values.

Definition of Site Effect

The potentially strong influence of site conditions has been known for almost 200 years. For example, waxing somewhat poetic on the 1811–1812 New Madrid sequence, Daniel Drake wrote:

> The convulsion was greater along the Mississippi, as well as along the Ohio, than in the uplands. The strata in both valleys are loose. The more tenacious layers of clay and loam spread over the adjoining hills . . . suffered but little derangement. (Drake, 1815, p. 82).

Site effects were also recognized in the great Japan earthquake of 1891 (Milne, 1898), the 1906 San Francisco earthquake (e.g., Wood, 1908), and the Long Beach earthquake of 1933 (Wood, 1933). The first quantitative study of sediment amplification in southern California was by Gutenberg (1957). Despite these early observations, the incorporation of site effects in hazard estimation remains somewhat crude. Part of the problem is the ambiguous meaning of site response.

Many studies divide the factors influencing earthquake ground motion into source, path, and site effects, a distinction that has proven useful for understanding and predicting seismic motion (e.g., Aki, 1988). It is important to keep in mind, however, that this distinction is ultimately artificial. For example, one might logically define a site as the extent of a sedimentary deposit; but this leads to problems when such deposits are several kilometers deep and bounded by earthquake-generating faults. For example, how should one distinguish between path and site effects for a fault that ruptures along the edge of the Los Angeles basin? Such ambiguities inevitably lead to arbitrary distinctions, such as the 30-m-depth cutoff used to characterize site conditions in current building codes (e.g., Dobry *et al.,* 2000). The practical importance of understanding site effects has fueled a great deal of research; the lack of a clear, absolute definition has led to a somewhat disparate body of literature on the topic. Nevertheless, the concept of site response is still useful provided the definition is clearly understood in any particular context.

Recall that the goal of PSHA is to consider all damaging earthquakes in a region. In this context, therefore, the site effect should be defined as the average behavior, relative to other sites, given all potentially damaging earthquakes. That is, because we don't know which earthquake will rupture next, we must average the site response over the variety of possible earthquake source locations. This will inevitably produce an intrinsic variability in the site response by virtue of different incidence angles, azimuths, and wave types. To warrant application of this average effect for microzonation purposes, the difference between sites must, to some extent, exceed the intrinsic variability at each site (Hudson, 1972; Aki, 1988).

It is also important that attributes used to define the site be readily available (e.g., in map form) or realistically obtainable, and that site factors be defined relative to the reference motion appropriate to whatever source-path model is being applied. For example, it would not be appropriate to apply a sediment-to-bedrock Fourier spectral ratio as a correction to a rock-site peak-acceleration attenuation relationship. In other words, given the ultimate ambiguity between path and site effects, the specification of one must be made in the context of the other.

Previous Research and Important Issues

In 1985 the USGS published a comprehensive report titled "Evaluating Earthquake Hazard in the Los Angeles Region: An Earth Science Perspective" (USGS, 1985). Included in this report were several articles related to site effects (Fumal and Tinsley, 1985; Joyner and Fumal, 1985; Rogers *et al.,* 1985; Tinsley and Fumal, 1985) including an overview by Borcherdt (1985). These articles represent an appropriate point of departure for the background discussion here, not only because they collectively constitute the first comprehensive treatment of site effects in southern California, but also because they identify several issues that remain salient today.

Empirical Site Response Estimates

From Nuclear Explosions. In one of the 1985 USGS articles, Rogers *et al.* (1985) presented empirical site-response estimates by applying the sediment-to-bedrock spectral-ratio technique pioneered by Borcherdt (1970). Because direct earthquake observations were limited to those of the 1971 San Fernando earthquake, most of their recordings were of underground nuclear explosions from the Nevada test site (Rogers *et al.,* 1979; Rogers *et al.,* 1984). After averaging results over three frequency bands, they applied statistical clustering techniques to determine which of several geotechnical parameters were most influential on site-response estimates. At frequencies above 2 Hz, they found near-surface void ratio (a proxy for shear wave velocity) to be most influential, with Holocene thickness and/or depth to basement influential as well. Below 2 Hz they found Quaternary thickness and/or depth to basement rock to be the controlling factors. They noted, however, that some of the factors are "highly interdependent" (Rogers *et al.,* 1985, p. 235), making it difficult to separate near surface effects from deeper basin effects. As discussed below, this problem continues to plague us today. Comparing nuclear-explosion data to recordings of the 1971 San Fernando earthquake, they also concluded that nonlinear site effects are negligible (also discussed later).

From Coda Waves. In a different approach, Su and Aki (1995) generated empirical site-amplification maps for southern California using the *S*-wave coda methodology developed by Aki and Chouet (1975), Tsujiura (1978), and Phillips and Aki (1986). One of the original motives for using coda waves was to take advantage of the relatively abundant vertical-component network data for which the corresponding direct *S*-wave arrivals are generally clipped. However, for PSHA, this approach is perhaps most appealing in that the coda is thought to be composed of scattered energy coming in from a variety of directions (Aki and Chouet, 1975), so the site-response estimates might naturally reflect an average over various source locations. Unfortunately, there is some disagreement on whether coda site-response estimates are consistent with the direct *S*-wave response; while some have found agreement between the two (e.g., Tsujiura, 1978; Kato *et al.,* 1995), others have not (e.g., Margheriti *et al.,* 1994; Seekins *et al.,* 1995; Bonilla *et al.,* 1997; Field 1996). Another concern is that the Su and Aki (1995) amplification factors are based on vertical-component network data and may not be applicable to horizontal-component motion.

From Ambient Noise. The use of ambient seismic noise (microseisms and/or microtremors) was also proposed to make up for the dearth of direct earthquake data. For example, Kagami *et al.* (1982) examined microtremor spectral ratios in the Los Angeles basin and found the amplitudes to correlate with depth to basement rock, nuclear explosions spectral ratio amplitudes of Rogers *et al.* (1979), and ratios obtained for the 1971 San Fernando earthquake. Kagami *et al.* (1986) found similar results from a more extensive set of observations carried out in the San Fernando Valley, and a two-dimensional, theoretical model was constructed by Navaro *et al.* (1990) which "shows a remarkable coincidence with the microtremor experimental data." In spite of these and other encouraging results (e.g., Yamanaka *et al.,* 1993), questions still prevail with respect to the applicability of ambient noise measurements (see Bard, 1998, for a review). As such, no microtremor-based amplification map has been forthcoming for the region. Regardless of whether such a map can be generated, array analyses of ambient noise data may still prove useful in determining subsurface structure (e.g., Aki, 1957; Okada, 1987; Yamanaka *et al.,* 1994).

From Recent Earthquake Data. The 1994 Northridge earthquake sequence finally provided the volume of digital data needed to make direct and widespread empirical estimates of earthquake site response in southern California. For example, Hartzell *et al.* (1996) inverted over 1,300 shear-wave recordings for site effects at 90 sites. Bonilla *et al.* (1997) did a similar analysis, but examined other site-response estimates as well, including horizontal to vertical ratios and coda amplification factors. In terms of *S*-wave amplification factors, both studies obtained spectral-ratio estimates effectively similar to those introduced by Borcherdt (1970), but by applying the generalized-inverse formulation of Andrews (1986). One reason for the latter approach is that many sediment sites in the region lack the nearby bedrock site needed to compute traditional spectral ratios. In the generalized-inverse approach, a simple path-effect correction is made, and the source and site effects are subsequently solved for simultaneously. The potential problem with such site effect estimates is that any difference between the true and assumed path effect will be mapped into the site response. Because all Northridge aftershocks emanate from the same main-shock region, this means that any regional focusing effects will contaminate the site-response estimates. Alternatively, we could include these regional effects in our definition of "site response", but then acknowledge that there will be some intrinsic variability among earthquakes throughout the region. Either way, the question remains as to whether such site-response estimates obtained from one earthquake (or aftershock sequence) will apply to those of another.

Harmsen (1997) performed a similar inversion for site response at 281 locations in the Los Angeles region using strong-motion records from the 1971 San Fernando, 1987 Whittier Narrows, 1991 Sierra Madre, and 1994 Northridge main shocks. In using these four earthquakes, Harmsen to some extent averaged over biases associated with each, at least at those sites where more than one earthquake was recorded.

Hartzell *et al.* (1998) combined the Northridge aftershock results of Hartzell *et al.* (1996) with the four main-shock results of Harmsen (1997) to produce a series of "First-Generation Site-Response Maps for the Los Angeles Region." These were obtained by contouring between all available sediment-site spectral-amplification values. As such, they represent the most comprehensive, empirically based site-amplification maps available for the Los Angeles region. Their 1–3 Hz map is reproduced here (Fig. 1). Note that it identifies several isolated locations with relatively high amplification values. The relevant question for PSHA is whether these will remain high for earthquakes other than those represented in the inversions, especially since no formal uncertainty estimates are provided. Nevertheless, the map does provide a model that can be tested against future data. In fact, one of the Phase III articles discussed below (Wald and Mori, 2000) compares the Hartzell *et al.* (1998) amplification factors with theoretical predictions based on borehole data.

Near-Surface Effects

As discussed by Joyner and Fumal (1985), seismological theory implies that ground motion should depend on near-surface conditions. For example, if losses due to reflec-

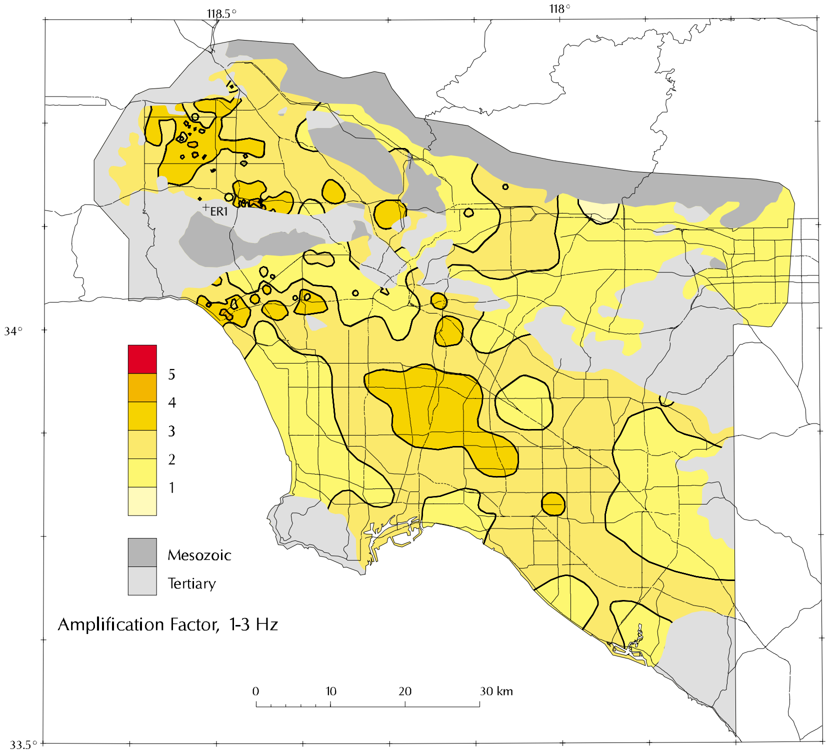

Figure 1. Empirical sediment-amplification map of Hartzell *et al.* (1998) for 1–3 Hz ground motion (modified from their Figure 4).

tion, scattering, and anelastic attenuation are negligible, then the energy along a tube of rays is conserved, and the amplitude is proportional to:

$$\frac{1}{\sqrt{\rho\beta}},$$

where ρ is density and β is shear-wave velocity (e.g., Bullen, 1965; Aki and Richards, 1980).

Because determination of density and seismic velocities requires costly geotechnical studies, one naturally looks to geology for a proxy. Most traditional geological maps were produced with mineral-resource development in mind, emphasizing differences in bedrock units while lumping sediments together. Recognizing this shortcoming for earthquake ground-motion estimation, Tinsley and Fumal (1985) developed detailed geological maps for the Los Angeles region. Most notably, they divided Quaternary alluvium into eight subunits on the basis of age ("young" Holocene versus "old" Pleistocene) and grain size (fine, medium, coarse, and very coarse). A version of the Tinsley and Fumal (1985) map, compiled and modified slightly by Park and Elrick (1998), is shown in Figure 2. This map remains one of the most detailed forms of Quaternary geological data available for the region. It therefore makes sense to relate relevant seismic parameters to each subunit.

Because density is relatively constant with depth, shear-wave velocity is the logical choice for representing site conditions. The question is how to reduce the depth-dependent velocity to a single, representative value. Joyner *et al.* (1981) proposed averaging the velocity over a depth range corresponding to one-quarter the wavelength of the period of interest. This generally produces frequency-dependent velocity values because longer wavelengths extend to, or sample, greater depths. By relating 1-Hz quarter-wavelength velocities inferred from 33 borehole sites to the detailed geology units of Tinsley and Fumal (1985), Fumal and Tinsley (1985) developed 1-Hz shear-wave velocity maps for the Los Angeles region.

The quarter-wavelength velocity is elegant in terms of having a physically based extent of depth averaging. However, most previous boreholes were limited to a depth of ~30 m, which corresponds to the extent of penetration achievable by a drill rig in a single day of operation, with a step-function increase in cost thereafter. This depth limitation generally precludes computation of the quarter-wavelength velocity over at least some frequencies of engineering interest. In fact, Fumal and Tinsley (1985) had to extrapolate borehole data in order to get the 33 values they applied.

An alternative is to compute the average velocity to a standard depth. For example, Tinsley and Fumal (1985) averaged velocities down to 30 m. This increased the number of average borehole velocities from 33 (under the quarter-wavelength definition) to 84. Using these values, they grouped like geological units together and thereby produced 30-m shear-wave velocity maps for the region.

Interestingly, the practical advantage of using average 30-m shear-wave velocity (referred to hereafter as V_{30}) has prevailed over the theoretical superiority of the quarter-

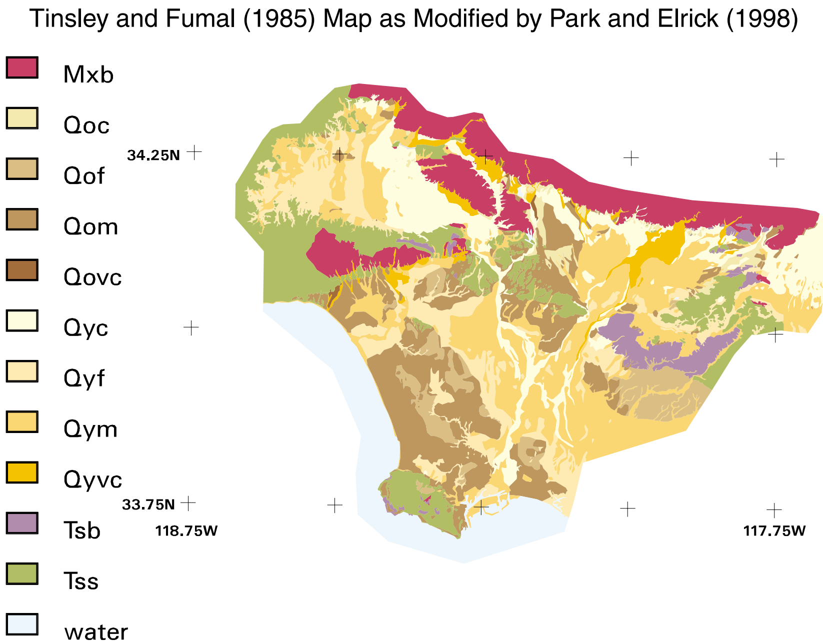

Figure 2. The detailed geology map of Tinsley and Fumal (1995) as modified by Park and Elrick (1998). Mxb, Mesozoic basement; Tss, is Tertiary sediment; Tsb, Tertiary basement. Q, Quaternary; o, old (Pleistocene); y, young (Holocene); and f, m, c, and vc for fine, medium, coarse, and very coarse grained, respectively. The modification of Park and Elrick (1998) was to add the Mxb, Tsb, and Tss units.

wavelength measure. Specifically, based on empirical studies (e.g., Borcherdt and Glassmoyer, 1992) and the recommendation of Borcherdt (1993, 1994), V_{30} was adopted as a means of classifying sites in the 1994 NEHRP building code provisions (BSSC, 1995). V_{30} has also been used to parameterize site effects in the attenuation relationships of Boore *et al.* (1993, 1997).

One might naturally question the validity of using V_{30} (or the quarter-wavelength velocity for that matter) when strong impedance contrasts exist. Such discontinuities will cause reflections from and/or reverberations within layers, thereby violating the conservation of energy arguments mentioned previously. However, assuming no anelastic attenuation, Day (1996) demonstrated theoretically that even if strong resonances exist, the response averaged over some finite-frequency bandwidth is still inversely proportional to $1/\sqrt{\rho\beta}$ averaged to some depth; the greater the depth, the greater the frequency resolution. Taken to the limit, this means that the response averaged over all frequencies (zero resolution) depends only on the velocity and density at zero depth. Considering this issue further, Anderson *et al.* (1996) found additional support for the use of V_{30}, but added that attenuation effects should be accounted for as well, especially at deeper sediment sites.

Basin Effects

Basin-Edge-Induced Waves. Examining displacement records from the 1971 San Fernando earthquake, Hanks (1975) noted that surface waves were prevalent in the Los Angeles basin. From an array analysis, Liu and Heaton (1984) demonstrated that these surface waves were converted from body waves along the basin edge. Vidale and Helmberger (1988) successfully modeled the behavior using two-dimensional finite-difference approach. A particularly good example of basin-edge induced waves (Fig. 3) was obtained in the Coachella Valley during the 1992 Landers earthquake aftershock sequence (Field, 1996). Although the initial *S* waves are amplified relative to bedrock, the largest amplitudes come from a wave that propagates across the valley from the northeastern edge (see caption for details). Interestingly, this area of the Coachella Valley had the largest level of shaking (outside the epicentral region) during the 2000 Hector Mine earthquake (Scientists from the USGS, SCEC, and

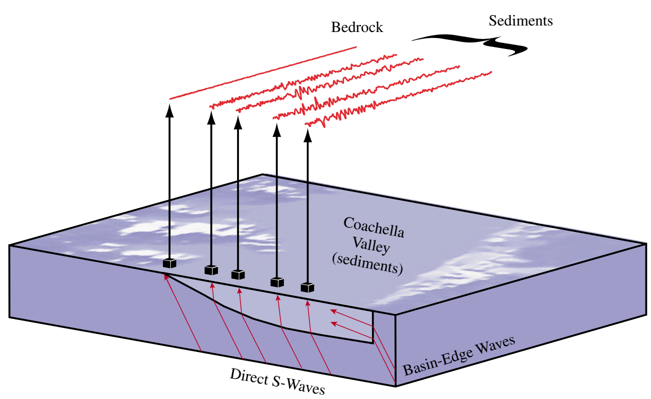

Figure 3. Basin-edge induced waves from a 1992 Landers earthquake aftershock observed in the Coachella Valley near Palm Springs, California (Field, 1996). The seismograms are of particle velocity and begin at the *S*-wave arrival. The largest ground motion at each valley site is produced by energy that has entered along the vertical edge of the basin. The ground motion on bedrock is almost imperceptible at this scale (the largest amplitude in the plot corresponds to ~0.2 cm/sec).

CDMG, 2000), presumably due to basin-edge-induced waves. This should not be surprising given the close juxtaposition of the Landers and Hector Mine ruptures. The relevant question with respect to PSHA is whether this part of the Coachella Valley will constitute a bright spot when the earthquake is in an entirely different location.

Subsurface Focusing. Another important basin effect is focusing caused by subsurface structure. Perhaps the most dramatic example of this was observed in Santa Monica during the Northridge earthquake sequence (Gao *et al.,* 1996). Aftershock recordings just 650 m apart exhibited peak-motion differences of up to a factor of 5 (Fig. 4). These differences generally correlate with the damage distribution of the main shock (Gao *et al.,* 1996). Such observations are at least 100 years old.

> It is an easy matter to select two stations within 1,000 feet of each other where the average range of horizontal motion at the one station shall be five times, and even ten times, greater than it is at the other (Milne, 1898).

However, modern studies are providing the physical explanation for this variability. A debate remains over whether the damage in Santa Monica resulted from the deeper (Gao *et al.,* 1996) or shallower (Alex and Olsen, 1998; Graves *et al.,* 1998) wedge structure depicted in Figure 4. Both explanations involve constructive interference, or focusing, of waves traveling different paths. As such, they both imply that the exact pattern of shaking will be sensitive to source location, a fact born out by the aftershock observations (Gao *et al.,* 1996). With respect to PSHA, this raises the question of whether the amplification pattern from the Northridge earthquake, or any site-effect map that is dominated by this earthquake (e.g., Fig. 1), is applicable to other events as well. It also raises the question of how much effort is warranted in determining the exact subsurface structure when the final result will be sensitive to the unknown locations, and perhaps even slip distributions, of future earthquakes.

Another case of subsurface focusing was documented by Hartzell *et al.* (1997) in Sherman Oaks, California. In fact, they concluded that " . . . sedimentary structures in the upper 1 to 2 km and topography on the sediment-basement interface . . . can be the dominant factor in the modification of local ground motion" (p. 1377). This also suggests that the amplification pattern will be somewhat, perhaps even largely, dependent on earthquake location.

Intrinsic Variability. The presence of basin-edge-induced surface waves and focusing effects does not bode well for predicting site effects in PSHA; it suggests that site response will have a large intrinsic variability with respect to source location. This would help explain several studies, in southern California alone, that identify large differences in earthquake shaking over hundred-meter distances (e.g., Steidl, 1993; Field and Hough, 1996; Hartzell *et al.,* 1996, 1997; Meremonte *et al.,* 1996), and that find ground motion to be sensitive to source location (e.g., Frankel, 1994; Hough *et al.,* 1995; Meremonte *et al.,* 1996; Scrivner and Helmberger, 1999). In fact, from 3D finite-difference simulations for a simplified San Andreas fault rupture, Frankel (1993) showed that the amplification pattern in the San Bernardino Valley is sensitive to the distribution of source asperities as well. Thus, not only is the separation of path and site effects somewhat vague and arbitrary, but so is the separation of source effects.

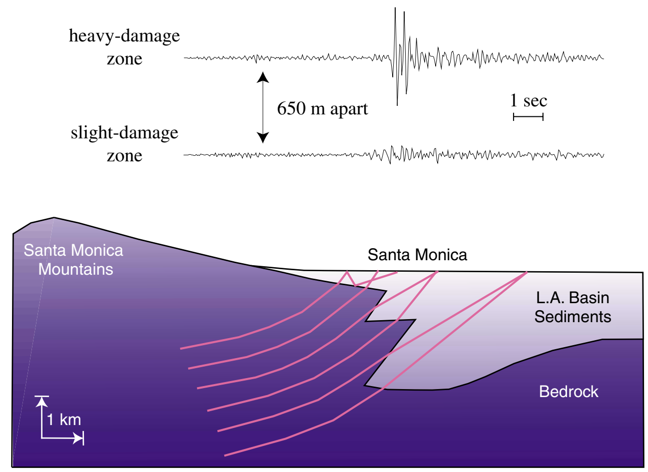

Figure 4. Particle-velocity seismograms (top) of a 1994 Northridge-earthquake aftershock recorded at two sites in Santa Monica, California, located just 650 m apart (from Gao *et al.,* 1996). The higher-amplitude seismogram corresponds to a location that suffered greater damage during the main shock. A cross section (bottom) adapted from Graves *et al.* (1998) illustrating how this difference may have resulted from a constructive interference, or focusing, caused by the subsurface basin structure (the rays are drawn for illustrative purposes only).

Average Behavior. Although an intrinsic variability of basin response with respect to rupture location seems inevitable, there may be some systematic behavior on average. Recall, for example, that Rogers *et al.* (1985) identified a correlation between spectral-ratio amplitudes and basin depth. In fact, this had been noted even earlier (e.g., Trifunac and Lee, 1978; Rogers *et al.,* 1979), and has been noted since (e.g., Campbell, 1987; Hartzell *et al.,* 1996; Hartzell *et al.,* 1998). For this reason, and as discussed below, considerable effort has gone into understanding a possible basin-depth effect in the Phase III collection of articles.

Nonlinear Site Effects

In the complications described previously, we have so far ignored the issue of sediment nonlinearity. To the extent that sediments yield at high levels of strain—a violation of Hooke's law resulting in a nonlinear response—amplification factors can be dependent on the ground-motion level (Reid, 1910). Because the vast body of literature on this topic has been reviewed elsewhere (e.g., Beresnev and Wen, 1996;

Field *et al.,* 1998a; Yoshida and Iai, 1998), only a very brief overview in the context of southern California is given here.

The engineering community has long believed that sediment nonlinearity is significant (e.g., Schnabel *et al.,* 1972). Their perspective is based largely on laboratory studies, where observed stress-strain loops imply a reduced effective shear modulus and an increased damping (lower Q) at higher levels of strain. On the basis of theoretical modeling, especially at the highest levels of shaking, the net effect is believed to be a reduction of amplification factors with increasing ground motion (e.g., Borcherdt, 1994). As discussed below, this perspective is reflected in the current generation of building codes (e.g., Dobry *et al.,* 2000).

Given a dearth of direct observations and a concern that laboratory studies may be misleading, seismologists traditionally have been skeptical of the significance of sediment nonlinearity. Their approach has been to adopt the simpler, linear model until data demand otherwise. For example, based in part on the work of Rogers *et al.* (e.g., 1995) discussed earlier, Aki's 1988 review article concluded that: " . . . except for the obvious case of liquefaction, . . . the amplification factor obtained using weak-motion data can be used to predict . . . strong ground motion . . . " (Aki, 1988, p. 115). Interestingly, Aki later became one of the earliest seismological converts, stating that: "Non-linear amplification at sediment sites appears to be more pervasive than seismologists used to think" (Aki, 1993). However, agreement among seismologists was not unanimous (e.g., Wennerberg, 1996; Chin and Aki, 1996), and skeptics maintained that documented cases were isolated and/or associated with liquefaction. This left the question open, especially for sediment conditions that typify southern California.

New data with which to test the nonlinearity issue were provided by the 1994 Northridge earthquake. For example, comparing weak- and strong-motion amplification factors, Field *et al.* (1997) concluded that nonlinear effects were statistically significant between approximately 1.0 and 5.0 Hz. Their results, reproduced in Figure 5, generally have been corroborated by other studies (e.g., Su *et al.,* 1998; Hartzell, 1998; and Beresnev *et al.,* 1998; Field *et al.,* 1998b). Thus, from a seismological perspective, sediments seemed to behave more nonlinearly during the Northridge earthquake than had been expected. From the engineering perspective, however, the Northridge data implied less nonlinearity than had been expected (e.g., Chang and Bray, 1997; Borcherdt, 1996).

Although results like those in Figure 5 allowed us to reject the null hypothesis that the response was linear, the averaging required to do so generally precludes a detailed understanding of the physics. In fact, according to a recent textbook on the topic, " . . . there is no nonlinear model of any kind established on a sound physical basis" (Ishihara, 1996, p. 28). This, coupled with a general lack of empirical data, suggests that we should expect some surprises. For example, one of the most widely used approaches for modeling sediment nonlinearity is the equivalent-linear formulation (Idriss Seed, 1968; Schnabel *et al.,* 1972), which generally predicts that as ground motion increases, the reduction in amplification will be greater at higher frequencies. However, Yu *et al.* (1993) applied a more explicit nonlinear model and found that high-frequency amplification factors can actually be increased (in direct contrast to an equivalent-linear prediction). Another surprising manifestation of nonlinearity is the presence of high-frequency spikes in some acceleration records (Zeghal and Elgamal, 1994; Archuleta, 1998; Bonilla *et al.,* 1998). These findings suggest that an open mind is needed as we sift through existing data and explore various theoretical models.

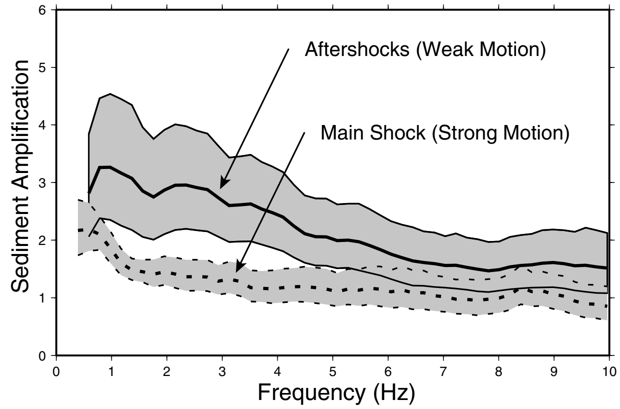

Figure 5. Comparison of strong- and weak-motion sediment-amplification factors for the 1994 Northridge earthquake (Field *et al.,* 1997). The dashed line is the average for the main shock, and the solid line is the average for aftershocks. A generalized inversion approach was used to estimate the site effects (e.g., Andrews, 1986), but the results are essentially equivalent to path-effect corrected sediment to bedrock spectral ratios. The averages were taken over 15 sediment sites, representing all that had both main-shock and aftershock records available, and four rock sites were used as the reference. The uncertainties represent approximately 95% confidence intervals for the mean.

It also should be noted that purely linear models can explain some observations that previously have been attributed to nonlinearity. For example, O'Connell (1999) argues that the discrepancy shown in Figure 5 can be explained by scattering alone. He suggests that waves from different parts of an extended fault sample different volumes of crust and therefore arrive less coherently than energy from small events. If the effect is more pronounced at sediment sites than at rock sites, we might expect the discrepancy seen in Figure 5. Two lines of reasoning are presented to support this contention. First, he shows that the inclusion of empirical scattering functions in synthetic seismograms reduces amplitudes by a factor of 1.82 on average (his Table 1). However, these simulations are for sediment sites only. To explain the discrepancy in Figure 5, it remains to be shown that the scattering effect is negligible at rock sites. Second, a series of 3D finite-difference proxy experiments were car-

Table 1
Site-Classification Scheme Defined in the 1994 and 1997 NEHRP Provisions (BSSC, 1995, 1998) and Applied in the 1997 Uniform Building Code

Class	V_{30} (m/sec)*	Description
A	>1500	Hard rock
B	760–500	Rock
C	360–760	Very dense soil and soft rock
D	180–360	Stiff soil
E	<180	Soft soil
F	Special soil requiring site-specific evaluation	

*V_{30} is the average shear-wave velocity in the upper 30 m at the site.

Table 2
F_a, The Short-Period (near 0.2 sec) Site-Correction Defined in the 1994 and 1997 NEHRP Provisions (BSSC, 1995, 1998) and Applied in the 1997 Uniform Building Code

Site Class*	$S_s \le 0.25$†	$S_s = 0.50$	$S_s = 0.75$	$S_s = 1.00$	$S_s \ge 1.25$
A	0.8	0.8	0.8	0.8	0.8
B	1.0	1.0	1.0	1.0	1.0
C	1.2	1.2	1.1	1.0	1.0
D	1.6	1.4	1.2	1.1	1.0
E	2.5	1.7	1.2	0.9	‡
F	‡	‡	‡	‡	‡

*The site classes are defined in Table 1.
†S_s is the short-period response spectral acceleration on rock. As specified in the NEHRP provisions, a straight line interpolation is applied for intermediate values of S_s.
‡A geotechnical investigation and dynamic analysis shall be performed.

ried out from which the author concluded that he could reproduce the 3-Hz empirical observations of Field *et al.* (1997). However, the comparison is not completely applicable in that his simulations were for peak acceleration, which is presumably more influenced by scattering than the Fourier-spectral observations of Field *et al.* (obtained from 20-sec windows). Nevertheless, he does point out a previously overlooked phenomenon that may be important, especially for peak-motion based attenuation relationships. More is said regarding nonlinear site response in the context of the Phase III articles below.

Site Amplification in Current Building Codes

The development and current use of site coefficients in building codes has been reviewed by Dobry *et al.* (2000). The 1994 and 1997 NEHRP provisions (BSSC, 1995, 1998), the 1997 Uniform Building Code (UBC), and the 2000 International Building Code (IBC) apply the classification scheme listed in Table 1, and the amplification factors listed in Tables 2 and 3. This overall approach was developed by consensus, based on empirical amplification factors at lower levels of shaking (rock PGA less than $\sim 0.1g$) and on numerical modeling of laboratory results at higher ground-motion levels (see Borcherdt, 1994, or Dobry *et al.,* 2000, for details). As discussed previously, the sites are classified according to the average 30-m shear-wave velocity (V_{30}). Separate amplification factors are given for short-period response near 0.2 sec (F_a in Table 2), and for longer-period response above 1.0 sec (F_v in Table 3).

In current building codes the amplification factors listed in Tables 2 and 3 are applied to the ground motion given in rock-site hazard maps. Strictly speaking, this approach is not valid if several different scenarios, with different implied ground-motion levels, contribute to the rock-site hazard (e.g., to the 2% in 50 years exceedance level). In such cases, a separate site correction should be applied to each event before computing the composite hazard. For practical purposes, however, applying a single, representative amplification factor to all events may be adequate, or all that is warranted, given our present understanding of nonlinearity.

Table 3
F_v, The Long-period ($\ge$1.0 sec) Site-Correction Defined in the 1994 and 1997 NEHRP Provisions (BSSC, 1995, 1998) and Applied in the 1997 Uniform Building Code

Site Class*	$S_1 \le 0.1$†	$S_1 = 0.2$	$S_1 = 0.3$	$S_1 = 0.4$	$S_1 \ge 0.5$
A	0.8	0.8	0.8	0.8	0.8
B	1.0	1.0	1.0	1.0	1.0
C	1.7	1.6	1.5	1.4	1.3
D	2.4	2.0	1.8	1.6	1.5
E	3.5	3.2	2.8	2.4	‡
F	‡	‡	‡	‡	‡

*The site classes are defined in Table 1.
†S_1 is the long-period response spectral acceleration on rock. As specified in the NEHRP provisions, a straight line interpolation is applied for intermediate values of S_1.
‡A geotechnical investigation and dynamic analysis shall be performed.

SCEC Phase III Studies

We now turn to the Phase III studies of how and if PSHA in southern California can be improved by accounting for site effects. For a site-effect correction in PSHA to be practical, it must be defined in terms of the average response given the multitude of earthquake scenarios considered in PSHA. The previous studies discussed earlier highlight several important issues. First, given the influence of basin-edge induced surface waves, subsurface focusing, and scattering in general, we should expect a large intrinsic variability in site response with respect to different earthquake locations. In spite of this variability, are there any average effects for which corrections can be made? A second important issue is sediment nonlinearity, which may produce amplification factors that depend on the level of input motion. As discussed by Dobry *et al.* (2000), the 1994 NEHRP site corrections applied in current building codes (Tables 2 and 3) provide an important standard that can be tested with additional information. Are these amplification factors consistent with our current understanding of site effects in southern California? Does it matter in terms of implied seismic hazard?

Because the distinction between path and site effects (and even source effects) is ultimately artificial, any site corrections must be made in the context of the entire model. With respect to PSHA, this means the site effect should be defined relative to whatever attenuation relationship is being applied. For this reason, most of the studies in this volume are focused on the development and/or evaluation of attenuation relationships. The Phase III articles in this issue can be categorized as follows:

Data (or Model Data) Compilations:

- The SCEC Phase III Strong-Motion Database, by Steidl and Lee (2000)
- The SCEC Southern California Reference Three-Dimensional Seismic Velocity Model Version 2, by Magistrale *et al.* (2000)
- A Site Conditions Map for California Based on Geology and Shear-Wave Velocity by Wills *et al.* (2000)

General Background Research:

- Evaluation of Methods for Estimating Linear Site-Response Amplifications in the Los Angeles Region, by Wald and Mori (2000)
- Site Amplification in the Los Angeles Basin from Three-Dimensional Modeling of Ground Motion, by Olsen (2000)
- Strong Motion from Surface Waves in Deep Sedimentary Basins, by Joyner (2000)
- Expected Shape of Regressions for Ground-Motion Parameters on Rock, by Anderson (2000)
- Expected Signature of Nonlinearity on Regression for Strong Ground Motion Parameters, by Ni *et al.* (2000)

Evaluation and Development of Attenuation Relationships:

- Evaluation of Empirical Ground-Motion Relations in Southern California, by Lee *et al.* (2000)
- Site Response in Southern California for Probabilistic Seismic Hazard Analysis, by Steidl (2000)
- Potential for Improving Ground-Motion Relations in Southern California by Incorporating Various Site Parameters, by Lee and Anderson (2000)
- A Modified Ground-Motion Attenuation Relationship for Southern California that Accounts for Detailed Site Classification and a Basin-Depth Effect, by Field (2000)

Test of Implications With Respect to PSHA:

- A Test of Various Site-Effect Parameterizations in Probabilistic Seismic Hazard Analyses of Southern California, by Field and Petersen (2000)

The above categorization is not generally used in the discussion of each article below. Rather, a more thematic narrative is followed.

Empirical Amplification Versus Theoretical Borehole Predictions

The article by Wald and Mori (2000) compares the site-specific empirical amplification factors of Hartzell *et al.* (1998, Fig. 1) with theoretical predictions based on borehole data. A total of 33 sites were available for the comparison, having both an observed value (not an interpolated value as in Figure 1), and borehole data within 290 m of the site. Three types of borehole-based predictions are examined: average 30-m shear-wave velocity (V_{30}); a quarter-wavelength amplification factor, which is proportional to the quarter-wavelength velocity discussed previously (Joyner *et al.,* 1981); and the complete vertically incident plane *S*-wave response predicted by the 1D, linear propagator-matrix method of Haskell (1960). The comparison is made for three frequency ranges (1–3 Hz, 3–5 Hz, and 5–7 Hz). Their result for 1–3 Hz, which generally shows the greatest correlation, is reproduced in Figure 6. Interestingly, V_{30} is better correlated with observed values than the quarter-wavelength or propagator-matrix amplification factors. This implies that V_{30} is a better predictive parameter, even though the other two are generally thought to be more accurate estimates. It would appear that the more elaborate approaches are not elaborate enough to be superior.

Although V_{30} at 1–3 Hz exhibits the highest correlation, a great deal of scatter remains. This could reflect uncertainties in the observed amplification factors, inadequacies in the predictions (e.g., the 1D and/or linear response assumption), a lack of exact colocation, or some combination of these. For example, applying a nonlinear model might increase the correlation by shifting the strong-motion predictions (open triangles) to lower values. Alternatively, there may be a large intrinsic variability in the response at each site, and there is not yet enough data to capture the average behavior (which in turn may or may not equal the borehole-based predictions in Figure 6). More analyses, and probably more data, are needed to resolve this issue. For now one should be prudent when applying the site-specific, empirical amplification factors of Hartzell *et al.* (1998), especially where interpolated via contouring in Figure 1. Similarly, one should recognize the potential inadequacies of any theoretical site-response prediction, especially in the context of the source-and path-effect model.

3D Finite-Difference Modeling of Basin Response

To make reliable predictions of basin response, one must have an accurate model of the subsurface structure. Version 2 of the SCEC 3D seismic velocity model of southern California is described in the article by Magistrale *et al.* (2000). The model consists of detailed, rule-based representations of the major southern California basins (Los Angeles basin, Ventura basin, San Gabriel Valley, San Fernando Valley, Chino basin, San Bernardino Valley, and the Salton Trough) embedded in a 3D crust over a variable depth Moho. Outside the basins the model is based on regional tomo-

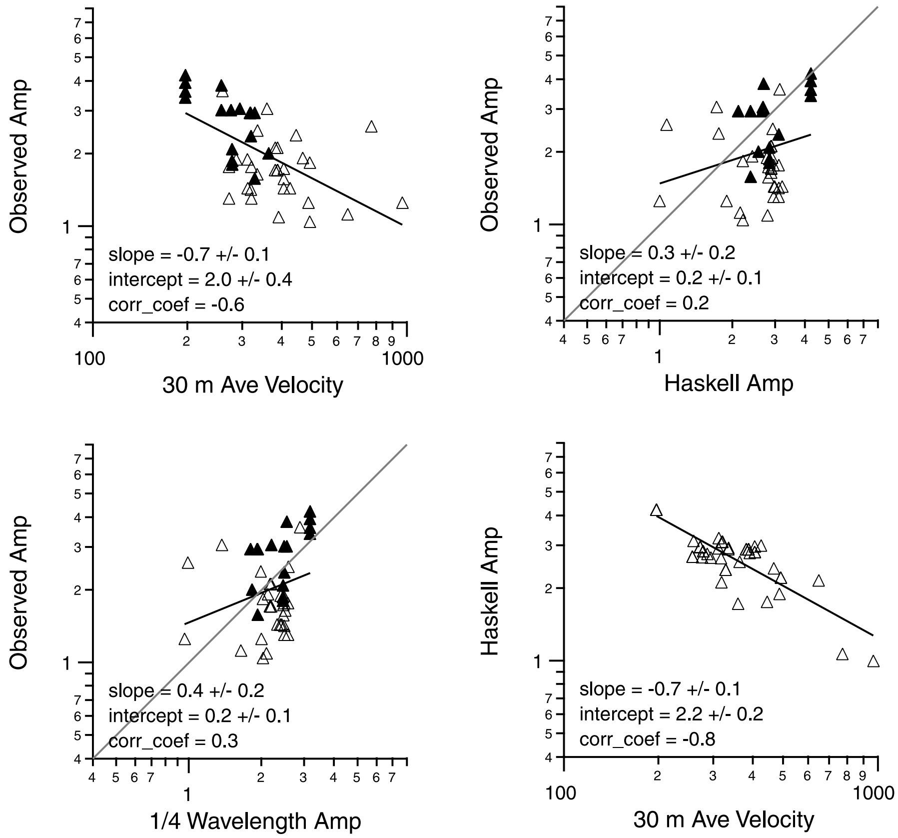

Figure 6. Comparison of various 1–3 Hz amplification factors obtained at 33 borehole sites (adapted from Figure 3 of Wald and Mori, 2000). The observed amplifications are all those from Hartzell *et al.* (1998) located within 290 m of a geotechnical borehole site. The 30-m average velocity, Haskell amplification, and quarter-wavelength amplification were all computed from the borehole data (see Wald and Mori, 2000, for details). The filled triangles represent weak-motion (aftershock) observations, and the open triangles are for strong-motion (main shock) observations.

graphic results, and Moho depths are determined from receiver-function analyses. Shallow basin sediment velocities are constrained by borehole data and the Wills *et al.* (2000) map of V_{30} (described in more detail later). The model is implemented in a computer code that generates any specified 3D mesh of seismic velocity and density values. A fence diagram of Magistrale *et al.* (2000) *S*-wave velocities is shown in Figure 7.

Recall that an important question is the intrinsic variability of basin response with respect to different earthquake source locations. Due to a present dearth of observations, this question must be addressed theoretically. The article by Olsen (2000) presents long-period (0–0.5 Hz) 3D finite-difference basin-response simulations for nine different scenario earthquakes. An earlier version of the Magistrale *et al.* (2000) structural model was used because the latter was not yet available (version 1 rather than version 2; see the individual articles for an exact description of the difference). The basin depth defined by the 2.5 km/sec shear-wave velocity isosurface for this model is shown in Figure 8, and the simulation results are shown in Figure 9. As a validation exercise, one of the simulations was for the 1994 Northridge earthquake. Figure 9 includes a comparison between predicted and observed peak velocities for this event (upper right). The agreement is generally within a factor of two.

The color maps in Figure 9 represent peak velocities for each simulated event, normalized by those from the same event in the background bedrock model. Each has also been normalized with respect to a 1D vertically propagating *S*-wave amplification factor. Thus, Figure 9 represents a reasonable attempt to isolate 3D basin effects for each event. Note that the amplification pattern varies greatly among the nine scenarios, implying a large intrinsic variability. In particular, the amplification pattern for the San Andreas fault differs depending on whether the rupture originates at the northwest or southeast end of the fault (bottom row in Figure 9). This sensitivity to the details of rupture is similar to what Frankel (1993) noted for the San Bernardino valley, and as previously mentioned, is an example of how the distinction between not only path and site effects, but also source ef-

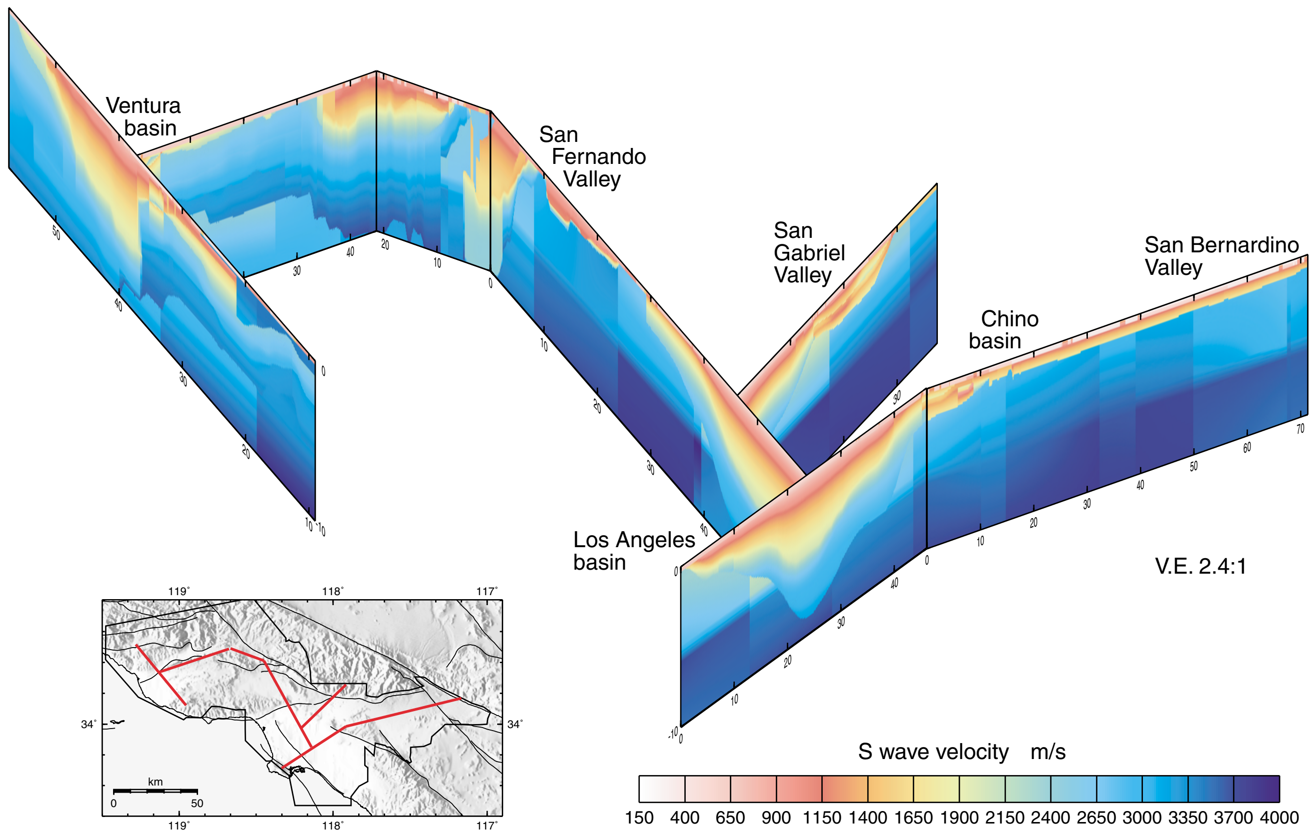

Figure 7. Fence diagram of shear-wave velocities in the Magistrale *et al.* (2000) 3D velocity model for southern California. This figure is an *S*-wave version of a similar plot they present for *P* waves.

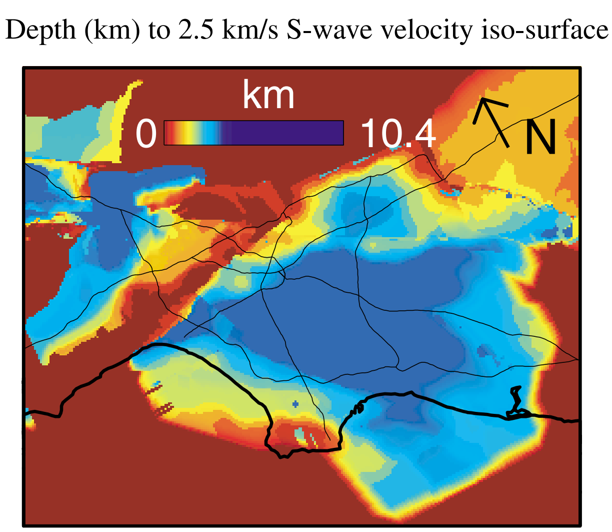

Figure 8. Depth to the 2.5 km/sec shear-wave velocity isosurface in the 3D model used by Olsen (2000). This is based on an earlier, and more geographically limited, version of the Magistrale *et al.* (2000) structural model, but the two are consistent.

fects, is ultimately artificial. The variability of amplification with respect to source location, let alone rupture, exacerbates the development of a generic amplification map. It again exemplifies how empirical estimates based on limited data (e.g., Fig. 1) may produce misleading results.

Given the large intrinsic variability in Figure 9, is there any systematic behavior that can be taken into account? As discussed previously, several studies have noted a correlation between the degree of amplification and basin depth. In fact, careful scrutiny of Figures 8 and 9 suggests such an effect. Figure 10 shows the average amplification versus depth (to the 2.5 km/sec shear-wave velocity isosurface) for each of the Olsen (2000) scenarios. Again, a large variability among events is observed, but a trend with basin depth is clear. The response averaged over all the earthquakes implies an amplification factor of about two at the deepest basin sites.

Wald and Graves (1998) have demonstrated that uncertainties in the basin model can have a significant effect on 3D ground-motion predictions. Therefore, one should be cautioned against overinterpreting the details of any simulation. However, the large intrinsic variability, and increase in average amplification with basin depth, are presumably robust inferences. Although the former is somewhat disap-

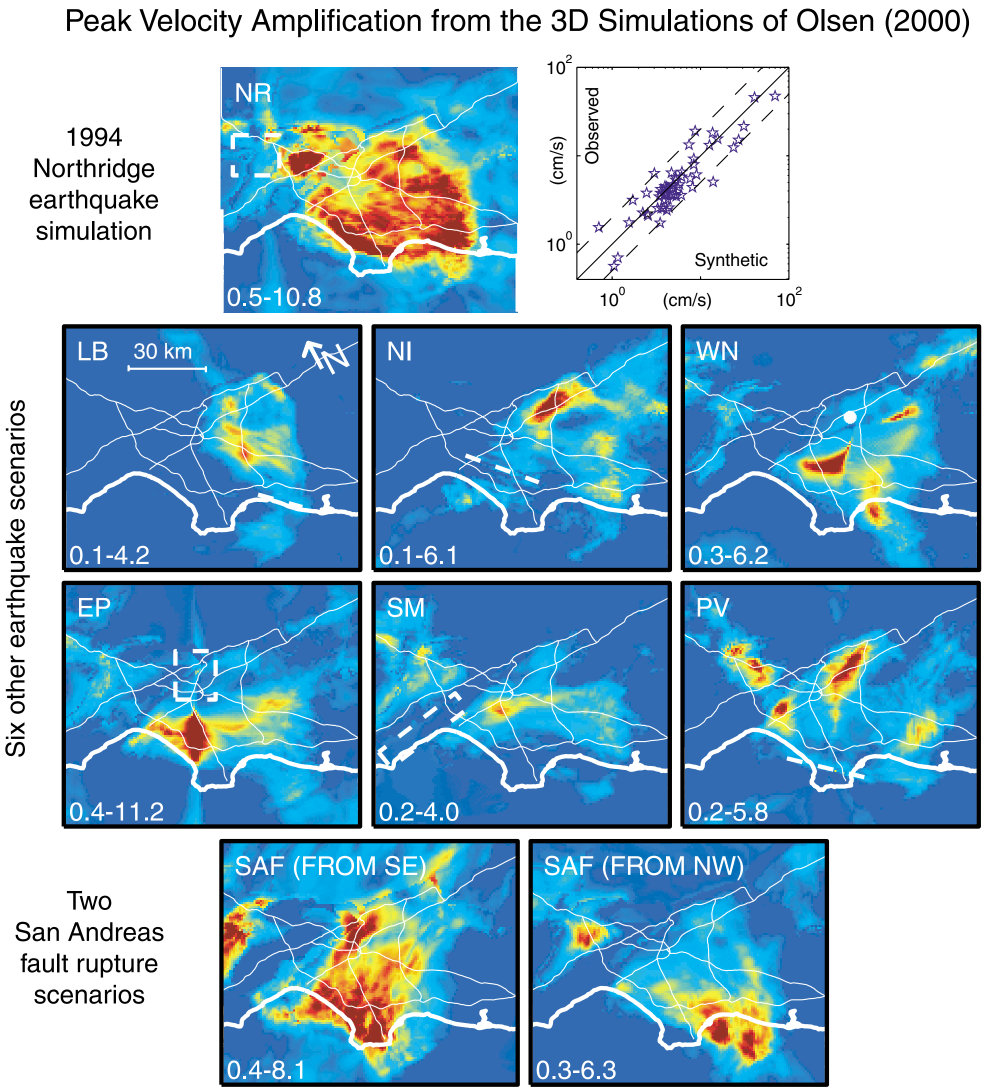

Figure 9. Peak velocity amplification pattern for nine different 0–0.5 Hz 3D finite-difference earthquake simulations (corrected for the 1D response at each site). The earthquake simulated in each plot is indicated in the upper left-hand corner (NR, 1994 Northridge; LB, Long Beach; NI, Newport Inglewood; WN, Whittier Narrows; EP, Elysian Park; SM, Santa Monica; PV, Palos Verdes; SAF (FROM SE) and SAF (FROM NW), San Andreas with rupture initiating from the southeast and northwest, respectively). The surface trace of the fault is plotted with a dashed white line (or dot), and the minimum and maximum amplification factor is given on the lower left. Also shown (upper right-hand plot) are predicted versus observed peak velocities for the 1994 Northridge earthquake. This figure is adapted from Figures 6 and 12 of Olsen (2000).

pointing in terms of predicting ground motion, the latter lends support to the notion that basin depth may be a useful parameter in earthquake hazard estimation.

Evaluation and Development of Attenuation Relationships and Their Implications with Respect to PSHA

We now focus on accounting for site effects in PSHA. Again, in the context of the source and path effect model, the question is how to appropriately modify an attenuation-relationship prediction. Therefore the remainder of the Phase III articles have concentrated on compiling new and relevant data, evaluating existing attenuation relationships, developing new attenuation relationships for southern California, and evaluating the implications of all relationships with respect to PSHA. Following Field and Petersen (2000), differences in ground motion that exceed 10% are referred to here as “important” because this is the threshold that typically influences engineering design. Similarly, “significant” is reserved for statistical statements at the one-sigma level (68% confidence), which is also customary in earthquake engineering.

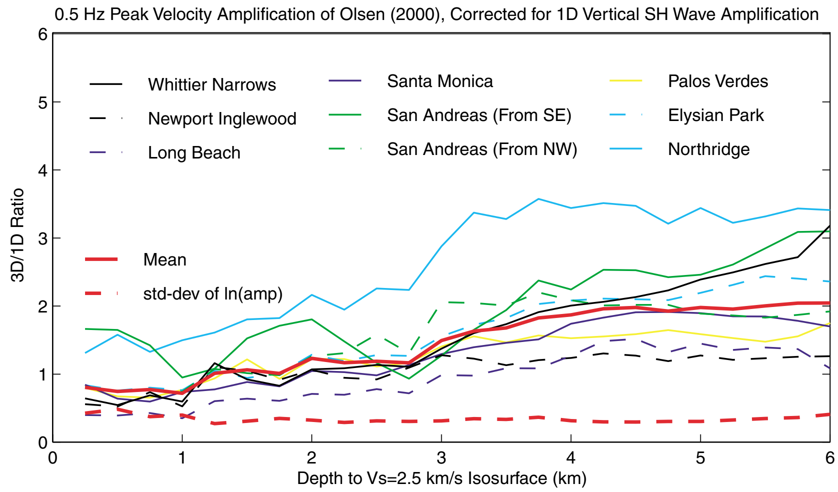

Figure 10. Average amplification for each of the Olsen (2000) 3D finite-difference scenario as a function of depth to the 2.5 km/sec isosurface. The average (red) and standard deviation of natural-log amplification (red-dashed) for all events are also plotted.

PSHA Basics. The goal of PSHA is to calculate the rate or probability of exceeding various levels of ground motion over a specified period of time, given all possible earthquakes in the region (Cornell 1968; Reiter, 1990). The two main components needed for the calculation are the source model and the attenuation relationship(s). Stated most simply, the source model specifies the magnitude, location, and probability of occurrence for all possible earthquakes in the region. The attenuation relationship gives an estimate of the ground motion at a site for a given earthquake. Specifically, it gives the mean and standard deviation for a ground-motion parameter (e.g., that natural log of PGA or response spectrum ordinate at a particular period), as a function of magnitude, distance, site type, faulting style, and sometimes, other parameters. The standard deviation, often referred to as sigma, reflects the inevitable imprecision or uncertainty associated with any model that strives to predict complex earthquake ground motion with so few parameters. This uncertainty is "aleatory" (dependent on chance) in that it reflects the intrinsic variability that cannot be reduced without changing the model (e.g., adding more parameters). An important question addressed below is whether this intrinsic variability can be significantly reduced with a more elaborate treatment of site effects.

For a given set of independent variables (i.e., magnitude, distance, site type, etc.), there is presumably a "true" mean and standard deviation of the ground-motion parameter for the entire population of events. The true values are, of course, unknown *a priori.* Rather, they are estimated from empirical or quasi-empirical data, usually by regression analysis assuming some analytical form. Many such attenuation relationships have been developed, several of which are documented in a special issue of *Seismological Research Letters* (1997, Volume 68, Number 1; see Abrahamson and Shedlock, 1997, for an overview). Attenuation relationships can differ in the following ways: (1) the assumed functional form; (2) the number and definition of independent variables; (3) the data selection/rejection criteria; and (4) the statistical treatment of sparse or unbalanced data. Given these choices, it is not surprising that different attenuation relationships often predict different levels of ground motion under equivalent conditions. Such disparities are referred to as "epistemic" uncertainties (related to a lack of knowledge) because additional studies and/or observations will eventually reveal the true mean and standard deviation for a given set of parameters.

Previously Published Attenuation Relationships. The article by Lee *et al.* (2000) evaluates five previously published attenuation relationships, each of which, being developed for shallow crustal earthquakes in active tectonic regions, should be applicable to southern California. These five relationships are listed in Table 4. To compare the predictions from the various relationships, one must adopt a consistent classification scheme. Lee *et al.* (2000) chose a Q/T/M categorization, based on Quaternary, Tertiary, and Mesozoic surface geology, because such information is readily available in map form (e.g., Park and Elrick, 1998) and can therefore be used for microzonation purposes. Table 4 shows how Lee *et al.* (2000) set the site parameters in each relationship to represent Q, T, and M. It should be noted that their designation may or may not agree with that of the original authors (reflecting a degree of judgement that is inevitable when applying someone else's relationship).

Figure 11, which shows the peak acceleration predicted by two of the attenuation relationships (Abrahamson and Silva, 1997; Boore *et al.,* 1997), exemplifies several important issues. Most dramatic is the relative difference between rock (M) and soil (Q) ground motion. The Boore *et al.* (1997) model has a sediment amplification that is constant with respect to magnitude and/or distance. The Abrahamson and Silva (1997) relationship, on the other hand, has a nonlinear amplification factor that varies with magnitude and distance, resulting in sediment deamplification at higher ground-motion levels. Other, more subtle differences between the two relationships include (1) the definition of distance from the fault (R_{jb} vs R_{rup}; see Abrahamson and

Table 4
The five attenuation relationships evaluated by Lee *et al.* (2000), along with how they set the site variables in each to represent Quaternary (Q), Tertiary (T), and Mesozoic (M) units

Attenuation Relationship	Q, T, and M Designation Defined by Lee *et al.* (2000)			Nonlinearity?*
Boore *et al.* (1997)	Q: V_{30} = 332 m/sec† T: V_{30} = 406 m/sec M: V_{30} = 569 m/sec			No
Campbell (1997)	Q: soil; basin depth = 2 km T: soft rock; basin depth = 2 km M: hard rock; basin depth = 0 km			Yes
Abrahamson and Silva (1997)	Q: deep soil T: rock M: rock			Yes
Sadigh *et al.* (1997)	Q: deep soil T: rock M: rock			Yes
Lee and Trifunac (1995)	Geol. Class	Soil Type	%Rock Path	
	Q: sediments	deep soil	90	No
	T: intermediate	stiff soil	95	
	M: basement	"rock" soil	100	

*Indicates whether the attenuation relationship, as defined, accounts for sediment nonlinearity (in terms of variable Q versus M amplitudes).
†V_{30} = average 30-m shear-wave velocity

Shedlock, 1997, for an overview of the various distance measures); (2) that the decay of ground motion with distance at rock sites is constant with respect to magnitude for Boore *et al.* (1997), but is magnitude-dependent in the Abrahamson and Silva (1997) model; and (3) that each not only has a different standard deviation (uncertainty), but that for Abrahamson and Silva (1997) depends on magnitude, whereas that for Boore *et al.* (1997) does not.

As discussed below, existing data provide limited resolution of the influence of sediment nonlinearity on attenuation relationships. Therefore, the Phase III study by Ni *et al.* (2000) has approached the issue theoretically. Specifically, they investigated the response of two hypothetical soil profiles to several hundred synthetic seismograms. The nonlinear constitutive properties of the soil were based on a standard geotechnical model (derived from laboratory studies), and the nonlinear response was computed using an explicit (as opposed to equivalent-linear) formulation. They found that peak-acceleration amplification factors are indeed decreased with increasing input ground-motion levels, with deamplification occurring above 0.2–0.4*g*. A similar result was found for 0.3–sec response spectra, with less of an effect (and no deamplification) observed at longer periods. The prediction is consistent with the behavior of the Abrahamson and Silva attenuation relationship (Fig. 11). However, it assumes that the laboratory-based constitutive model is applicable to *in situ* conditions. In addition, other physical mechanisms, such as the scattering hypothesis of O'Connell (1999), might explain the same behavior.

Similarly, Anderson (2000) has addressed theoretically the question of whether the decay of amplitude with distance depends on earthquake magnitude. Using three different synthetic-seismogram simulation techniques, he finds that ground motion decays less rapidly with distance for larger magnitude earthquakes. Intuitively, this result suggests that at larger distances, and for larger earthquakes, there is more opportunity for constructive interference of scattered arrivals from various subevents on the fault. Again, this prediction is consistent with the behavior of the Abrahamson and Silva (1997) attenuation relationship, but is also dependent on various assumptions made in computing the synthetic seismograms.

The differences just discussed regarding the two attenuation relationships shown in Figure 11 are just a few of several that exist among the five attenuation relationships listed in Table 4. However, it is beyond the scope of this overview article to discuss all such differences in detail. In fact, such a discussion would likely be more confusing than enlightening. Instead, we focus on the differences that significantly influence seismic hazard (i.e., the probability of exceeding various ground-motion levels), as quantified in the article by Field and Petersen (2000).

There is an overwhelming number of factors that influence a seismic-hazard estimate, including the source model, ground-motion parameter, site location, site type, and attenuation relationship(s) chosen. To keep the volume of results manageable, Field and Petersen (2000) narrowed these degrees of freedom considerably. For example, only a single regional source model, developed by CDMG and the USGS (Petersen *et al.,* 1996; Frankel *et al.,* 1996), was applied, which having been used to generate their national hazard maps, represents the closest thing to a standard model for southern California. In keeping with other Phase III studies, the analysis was carried out for four ground-motion parameters: peak horizontal acceleration (PGA), and 0.3-, 1.0-, and 3.0-sec response spectral acceleration (SA) with 5% damping. Hazard curves, which give the rate of exceeding various ground-motion levels, were reduced to a single value by selecting the ground motion that is exceeded every 475 years on average (corresponding to the level that has a 10% chance of being exceeded in 50 years, referred to hereafter as the 10%-in-50 yr exceedance level). However, Field and Petersen (2000) show that conclusions regarding the influence of site effects should be applicable to 2%-in-50 yr and 40%-in-50 yr exceedance levels as well. Finally, they restricted their analysis to 43 representative sites extending along a profile from Palos Verdes, across the Los Angeles basin, over the San Gabriel Mountains, and into the Mojave Desert (Fig. 12). Even with these restrictions, more than 10,000 exceedance values were generated in testing the various attenuation relationships and associated site-effect parameterizations. To maintain brevity, only representative examples from the Field and Petersen (2000) analysis are presented here.

Figure 13 shows the PGA 10%-in-50 yr exceedance val-

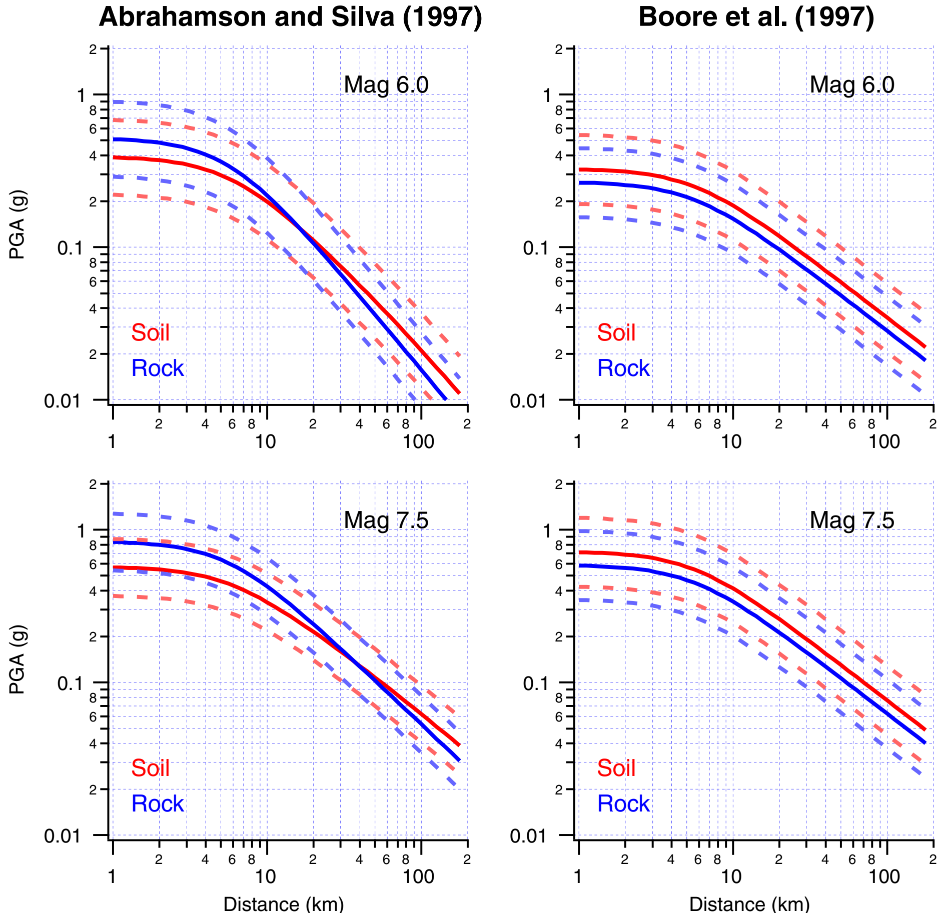

Figure 11. PGA curves for vertically oriented, surface rupturing, strike-slip earthquakes predicted by the Abrahamson and Silva (1997) and Boore *et al.* (1997) attenuation relationships (the different distance measures used in each, R_{jb} versus R_{rup}, are equivalent for this case). The solid lines are the median values and the dashed lines represent plus and minus one standard deviation (sigma).

ues along the profile for the two attenuation relationships shown in Figure 11 (the Boore *et al.,* 1997, and Abrahamson and Silva, 1997, relationships). Separate lines are shown assuming Q, T, and M site conditions along the entire profile (rather than assigning the actual site category). The three prominent peaks in Figure 13 at 7 km, 60 km, and 90 km along the profile correspond to events on the Palos Verdes ($6.5 \leq M \leq 7.1$), Sierra Madre ($6.5 \leq M \leq 7.0$), and San Andreas faults (M 7.8), respectively.

Note in Figure 13 that the Q exceedance values are always greater than those for M in the Boore *et al.* (1997) relationship, but that the M values generally exceed the Q values for the Abrahamson and Silva (1997) relationship. This discrepancy reflects the differing assumptions noted earlier regarding the influence of sediment nonlinearity. While the amplification factors of Boore *et al.* (1997) are constant (linear), those of Abrahamson and Silva (1997) depend on the PGA predicted for rock-site conditions (which in turn depends on magnitude and distance).

Recall that the 10%-in-50 yr ground-motion level depends, to some degree, on all events represented in the source model. However, it is often the case that only one or a few of the scenarios dominate the hazard, such as near the peaks in Figure 13. Understanding which earthquakes are influential is key to assessing why different attenuation relationships predict different hazard levels. The process of identifying the magnitude(s) and distance(s) associated with the dominant earthquake(s) is known as disaggregation (McGuire and Shedlock, 1981; McGuire, 1995; Cramer and Petersen, 1996; Bazzurro and Cornell, 1999). The values obtained depend not only on the site location, ground-motion parameter, source model, and attenuation relationship applied, but also on how the dominating values are measured (e.g., the median, mode, or mean of the distribution of events). For the sake of brevity, we simply state here that the 10%-in-50 yr exceedance levels across the profile of sites in Figure 12 are generally dominated by $M \geq 6.75$ events within ~20 km of the site. There are, of course, some exceptions, but the statement is accurate enough for present purposes (see Field and Petersen, 2000, for details).

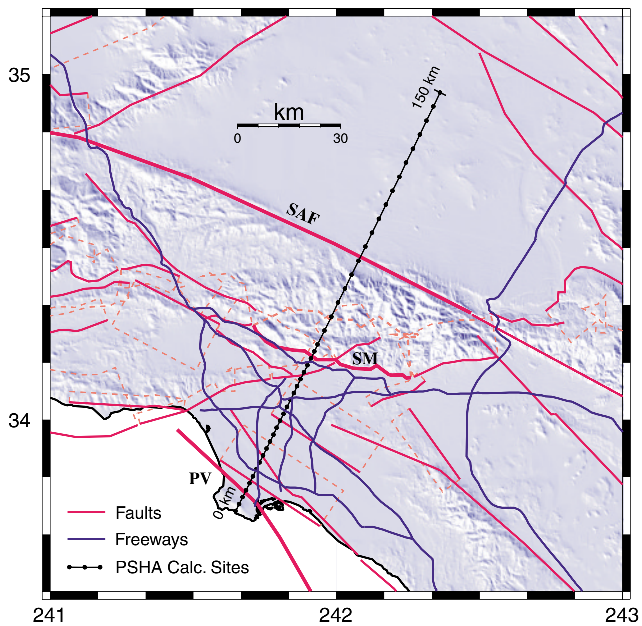

Figure 12. Map showing the profile of sites (black circles) where PSHA calculations were computed by Field and Petersen (2000). The top edge of each fault in the source model is plotted in red, with the down-dip extension dashed. Freeways are shown with blue lines. The Palos Verdes (PV), Sierra Madre (SM), and San Andreas (SAF) faults are plotted with wider lines.

Clearly the reliability of a hazard estimate depends on the reliability of the attenuation-relationship prediction at the dominant magnitudes and distances ($M \geq 6.75$ within $\sim$20 km here). For example, the Abrahamson and Silva (1997) attenuation relationship predicts sediment deamplification for PGA under these conditions, whereas the Boore *et al.* (1997) relationship predicts amplification (Figs. 11 and 13). This discrepancy reflects a problem that presently permeates hazard estimation: the conditions that dominate hazard (e.g., shaking in close proximity to large earthquakes) correspond to those where attenuation relationships are least constrained by data.

Figure 14 shows the 10%-in-50 yr PGA hazard values across the profile of sites for all five attenuation relationships listed in Table 4, along with the mean and standard deviation (computed from natural-logarithmic values). Note that the site category (Q, T, or M) specific to each site has been applied in this figure. There is up to a factor of 3 difference among the 10%-in-50 yr exceedance levels implied by the five relationships in Figure 14, and up to a factor of two difference relative to the mean. The differences exhibited in Figure 14 are therefore important (>10%). They reflect epistemic uncertainties in that a true 10%-in-50 yr exceedance level presumably exists, and each of the predictions in Figure 14 constitutes an estimate. The customary practice is to average results obtained with various attenuation relationships (e.g., SSHAC, 1997). Interestingly, averaging the PGA exceedance levels for the five attenuation relationships in Table 4 removes any significant difference between Q and M (because of differing opinions on whether Q is amplified or deamplified relative to M). However, for 1.0- and 3.0-sec SA the differences between Q and M are significant (see Figure 3 of Field and Petersen, 2000).

The practice of averaging over the different hazard levels predicted by various attenuation relationships will not reveal the true hazard if all relationships are similarly biased to begin with (for example, by relying on a similar limited observational database). It should again be noted that the results in Figure 14 relate to the particular Q/T/M implementation outlined in Table 4, which may or may not agree with how others (including the original authors) would have applied each relationship.

Southern California Strong-Motion Database. The ultimate test for any attenuation relationship is how well it predicts empirical observations. Steidl and Lee (2000) have compiled a southern California strong-motion database for the purposes evaluating and developing attenuation relationships. The distribution of magnitudes and distances represented in this database is shown in Figure 15. As with any database, its use for evaluation and developmental purposes implicitly assumes that it is representative of long-term, average behavior. All of the attenuation relationships listed in Table 4 were developed using less regionally restrictive sets of observations. The hope here is that by focusing on the southern California database exclusively, we will learn something unique about the region and not be led astray by data limitations. The southern California focus is also necessary to evaluate the predictive capability of attributes associated with, for example, the 3D regional velocity model of Magistrale *et al.* (2000). Furthermore, even with its geographical limitation, the database of Steidl and Lee (2000) contains more observations than were used in developing some of the previous relationships (e.g., Boore *et al.,* 1997).

Lee et al. *(2000) QTM Corrections to Previous Relationships.* The study by Lee *et al.* (2000) includes an evaluation of the five attenuation relationships listed in Table 4 with respect to the southern California strong-motion database (Steidl and Lee, 2000). Specifically, they computed a Q, T, and M bias for each relationship, which can be used as a southern California correction factor. They also computed an alternative magnitude-dependent sigma estimate (prediction error or standard deviation) for each relationship using the southern California data. Applying both of these as a correction to the five previously published relationships, Field and Petersen (2000) obtained the PSHA results shown in Figure 16 (which is analogous to Figure 14, but with the corrections applied). The differences between results in Figures 14 and 16 are due not only to the bias corrections, but also to differences in sigma as well.

Depending on the ground-motion parameter, typical values of sigma are $\sim$0.4 to $\sim$0.8 (for the natural log of ground motion). As discussed by Field and Petersen (2000), and shown in their Appendix Figure 6, changing sigma by

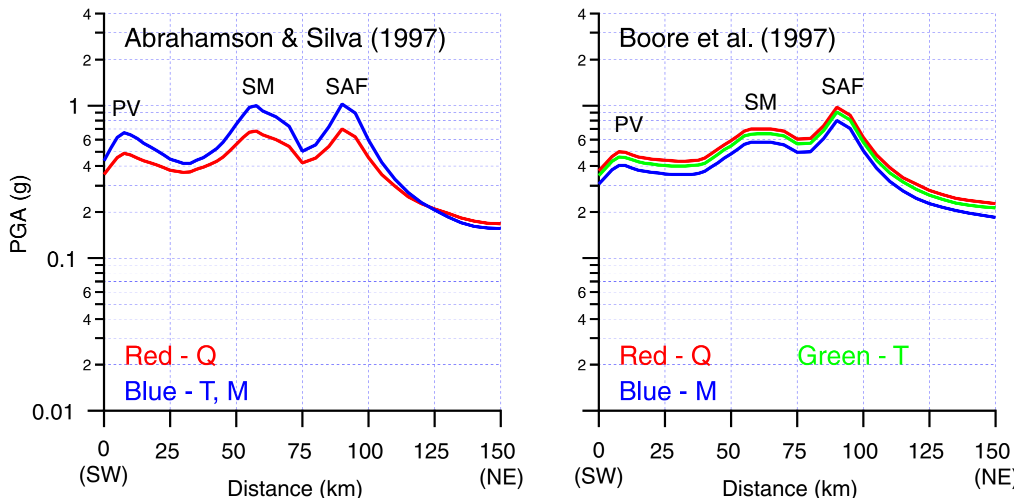

Figure 13. 10%-in-50 yr PGA predicted by applying the Abrahamson and Silva (1997) and Boore *et al.* (1997) attenuation relationships for the profile of sites shown in Figure 12. Results are shown separately for Q, T, and M site conditions (as defined in Table 4) along the entire profile. The prominent peaks at 7 km, 60 km, and 90 km correspond to the Palos Verdes (PV), Sierra Madre (SM), and San Andreas faults (SAF), respectively. This figure was adapted from those in Field and Petersen (2000).

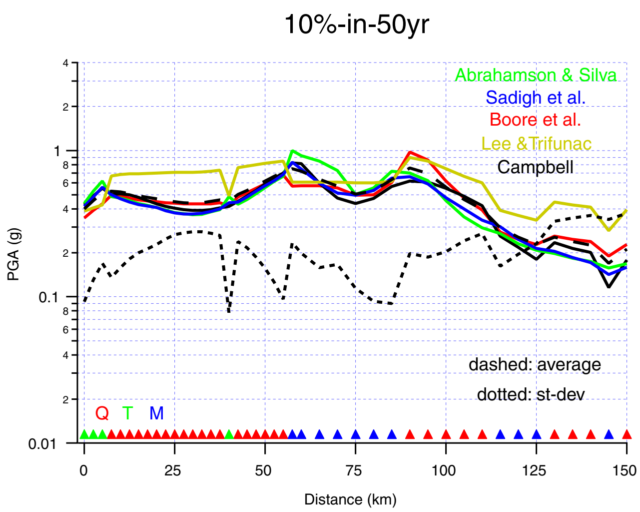

Figure 14. 10%-in-50 yr PGA predicted by all five attenuation relationships listed in Table 4, for the profile of sites shown in Figure 12. Here, the Q, T, or M site condition specific to each location has been assigned. The dashed line is the geometric mean, and the dotted line is the standard deviation computed from natural log values for the five estimates. This figure was adapted from those in Field and Petersen (2000).

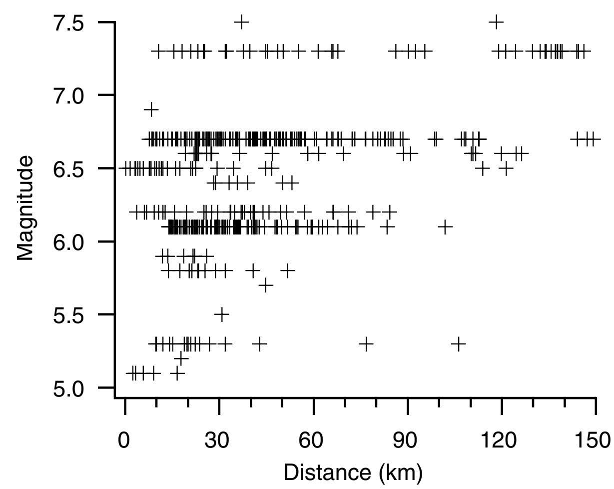

Figure 15. Magnitude versus distance (R_{rup}, as defined in Abrahamson and Shedlock, 1997) for all observations represented in the SCEC strong-motion database (Steidl and Lee, 2000).

more than about ± 0.1 causes a 10% change in the 10%-in-50 yr exceedance level. Thus, a useful rule of thumb in this study (but not necessarily applicable elsewhere) is that changing sigma by more than ± 0.1 will produce an important difference in terms of influencing engineering design. Increasing sigma increases the hazard (all other things being equal), because higher ground motions become more probable. Most of the Lee *et al.* (2000) sigma values are greater than those originally published, indicating that southern California observations are more variable than those used in the original studies (see Table 5 of Field and Petersen, 2000).

Applying both the southern California bias and sigma corrections of Lee *et al.* (2000) produced a more than 10% change in the 10%-in-50 yr exceedance level (under at least some conditions) for all five relationships in Table 4 (Field and Petersen, 2000). Because all are based on the same data, one might expect the corrections to bring the probabilistic ground-motion levels predicted by the five relationships into better agreement. This is indeed sometimes true, as the vari-

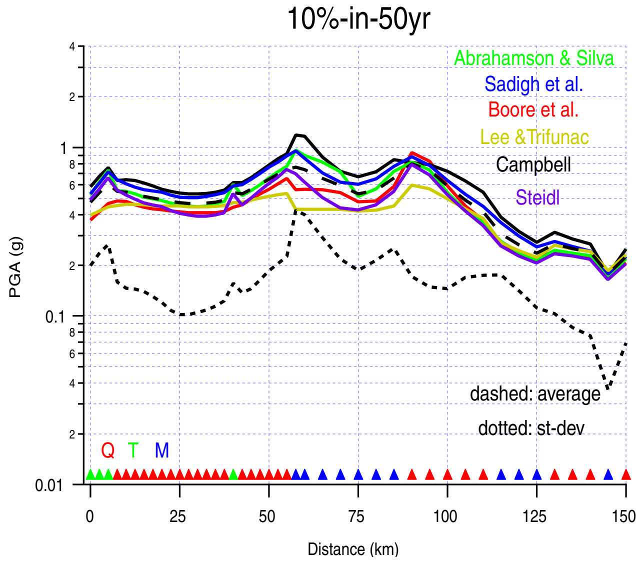

Figure 16. Similar to Figure 14, but where the southern California Q/T/M bias and sigma correction of Lee *et al.* (2000) has been applied to each relationship in the PSHA calculations. Also shown are the values predicted by the Steidl (2000) QTM relationship (purple line), which were not included in computing the mean and standard deviation of the other five estimates. This figure was adapted from those in Field and Petersen (2000).

ability among Q-sites is lower in Figure 16 than it is in Figure 14 (compare dotted lines). However, there are cases where the corrections increase the variability among the 10%-in-50 yr exceedance levels (e.g., M-site results between Figures 14 and 16). This can be explained as follows. The Lee *et al.* (2000) corrections are based on the southern California strong-motion database, for which the average magnitude and distance are ~6.4 and 40 km, respectively (Figure 15). Making the corrections will presumably cause the attenuation relationships to agree more at this magnitude and distance. However, because these are not the exact same magnitudes and distances that are dominating the hazard ($M \geq 6.75$ within ~20 km), there is no guarantee that the corrections will make the 10%-in-50 yr exceedance levels agree more.

The question then becomes whether forcing agreement at the average magnitude and distance represented in the database will make the predictions more reliable at the conditions dominating the hazard. Stated differently, a bias at one magnitude and/or distance does not necessarily mean the attenuation relationship is biased at another magnitude and/or distance. Furthermore, there is no guarantee that the present southern California strong-motion database is representative of the average, long-term behavior. Because answers to these questions are presently unknown, it is difficult to argue for the superiority of the corrected relationships. As attenuation relationships are almost constantly undergoing revision, the results of Lee *et al.* (2000) would probably serve better as a guide to authors as they update their models.

Steidl (2000) Attenuation Relationship. Steidl (2000) developed an attenuation relationship for southern California by computing empirical amplification factors (and new sigma estimates) relative to the Sadigh (1997) rock-attenuation relationship. The amplification factors at each period depend on the predicted rock-site PGA in order to allow nonlinear site effects. These were obtained by averaging residuals between observed and predicted values for Q, T, and M sites separately, and over different predicted rock PGA bins (PGA $\leq 0.05g$; $0.05 <$ PGA ≤ 0.1; $0.1 <$ PGA ≤ 0.2; and $0.2 <$ PGA). The PGA results for Q and M are shown in Figure 17. The average residuals (or log-amplification-factors) decrease with increasing predicted rock PGA. This would suggest nonlinear amplification if the trend existed only for Q sites. However, there is also a trend for M sites, suggesting a possible problem with the Sadigh (1997) relationship (in the magnitude and/or distance dependence). To demonstrate nonlinearity, therefore, it is necessary to divide the Q amplification factors by the M amplifications factors (to remove the magnitude and/or distance biases). Doing so produces equivocal results, mostly because a limited number of high ground-motion rock-site observations give rise to very large uncertainties. In fact, Steidl (2000) attempted to explicitly test the NEHRP amplification factors listed in Tables 2 and 3, but there were only two M-site observations (needed to normalize the Q-site results) in the three highest bins combined.

In spite of the potential problems with the Sadigh (1997) relationship and ambiguities regarding the significance of nonlinearity, the Steidl (2000) attenuation relationship remains viable. As can be seen from Figure 16, the 10%-in-50 yr PGA exceedance levels predicted by this relationship are generally consistent with the others. However, it is interesting to note that because relatively large ($M \geq 6.75$) magnitude events at short distances ($< \sim$20km) dominate the hazard, only the amplification factors for the highest ground-motion bin (rock PGA > 0.2g) are effectively applied (Field and Petersen, 2000). Thus, we again face the issue that the hazard calculations are most dependent on conditions least represented in the data.

Finally, it should be noted that Steidl also examined the following: (1) a subclassification of Q based on the detailed geology map of Tinsley and Fumal (1985); (2) a trend in residuals with respect to shear-wave velocity (V_{30}) obtained within 1 km of the observation site; and (3) a trend in residuals with respect basin depth. These results are generally consistent with those of Lee and Anderson (2000) and Field (2000) discussed subsequently.

Lee and Anderson (2000) Attenuation Relationship. Lee and Anderson (2000) customized the Abrahamson and Silva (1997) attenuation relationship by evaluating prediction residuals relative to southern California observations. Their

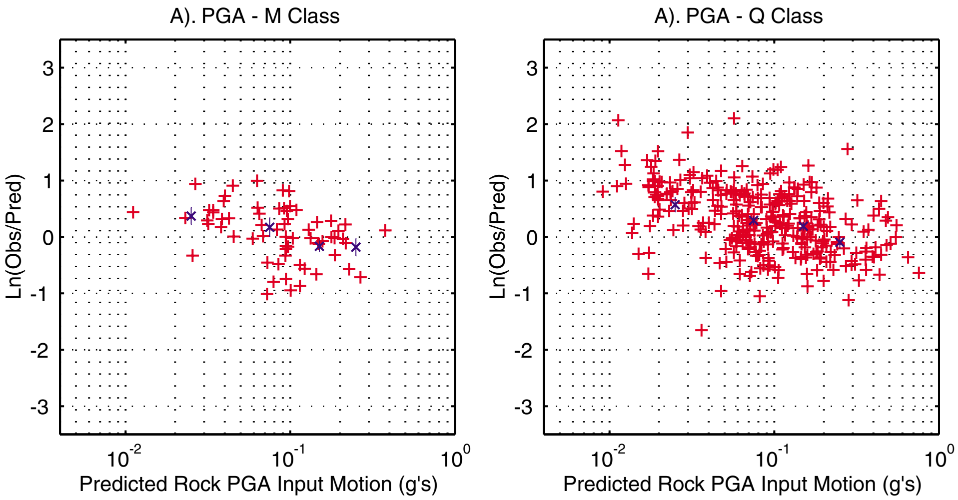

Figure 17. M- and Q-site PGA residuals of observed southern California data, relative to the Sadigh rock-site prediction, plotted versus the rock-site prediction (from Steidl, 2000). Individual values are shown in red, and blue symbols represent averages computed over four bins (PGA $\leq 0.05g$; $0.05 <$ PGA ≤ 0.1; $0.1 <$ PGA ≤ 0.2; and $0.2 <$ PGA). The vertical bars on the averages represent plus and minus one standard deviation of the mean.

approach differs from that of Steidl (2000) in that residuals for sediment sites are computed relative to the deep-soil (rather than rock) prediction. Thus, the sediment site residuals already have a first-order, nonlinear site-effect correction. They examined whether residuals are significantly correlated with the following site attributes: amplification predicted from weak-motion aftershock studies; low-frequency amplification predicted from 3D finite-difference simulations (Olsen, 2000); kappa from weak-motion studies (Anderson and Hough, 1984); basin depth (Magistrale *et al.,* 2000); and the detailed geological classifications of Tinsley and Fumal (1985), as modified by Park and Elrick (1998).

Figure 18 shows their average detailed geology residuals for PGA and 1.0-sec SA. Two of the Q subcategories (Qym and Qom) are both significant (at 68% confidence) and important (amplification greater than 10%) for PGA. However, neither is significantly different from the other Q subclassification residuals. None of the 1.0-sec SA results are significantly different from zero at the 68% level of confidence. Furthermore, there is no consistent trend with respect to the subunit age or grain size. For these reasons Lee and Anderson (2000) do not recommend application of their detailed geology corrections.

Of all the site attributes examined, basin depth produced the most unique and statistically significant trends (with depth, again, being defined relative to the 2.5 km/second shear-wave velocity isosurface in Figure 8). The amplification factors implied by their basin-depth corrections are shown in Figure 19 for the profile sites where depth is known (traversing near the deepest part of the Los Angeles basin). Relative to zero-depth, which exhibits some deamplification, the deepest basin sites are amplified by factors of ~1.5 for PGA and ~1.8 for 1.0-sec SA.

Lee and Anderson (2000) found that making the basin-depth and detailed geology corrections does not significantly reduce sigma (the prediction error, or standard deviation). In fact, they recommend using the sigma values published originally by Abrahamson and Silva (1997). For this reason, the effect of applying their basin-depth correction is to multiply the Abrahamson and Silva 10%-in-50 yr exceedance estimates by the amplification factors in Figure 19 (obviating the need to redo the PSHA calculations). Doing so has a statistically significant and important influence on hazard levels for all four ground-motion parameters (PGA, and 0.3-, 1.0-, and 3.0-sec SA).

Wills et al. *(2000)* V_{30} *Map.* As discussed previously, both Steidl (2000) and Lee and Anderson (2000) found that use of the detailed geology map of Tinsley and Fumal (1985) is not warranted for microzonation purposes. Following completion of those studies, a new detailed site-classification map was made available by Wills *et al.* (2000). This map, reproduced in Figure 20, uses the 1994 NEHRP classification scheme adopted in the 1997 UBC and 2000 IBC, with site types A, B, C, D, and E based on the average shear-wave velocity in the upper 30 m (Table 1). The map was compiled from 1:250,000 scale geology maps by combining similar units, and correlating these with *in situ* shear-wave velocity measurements where available (they did not use the map of Tinsley and Fumal, 1985). Because many geological units had shear-wave velocities that fell near the boundaries of the NEHRP categories, Wills *et al.* (2000) included intermediate categories as well (BC, CD, and DE). In addition to being directly tied to the building codes, the map has the advantage of covering the entire state of California, whereas the Tinsley

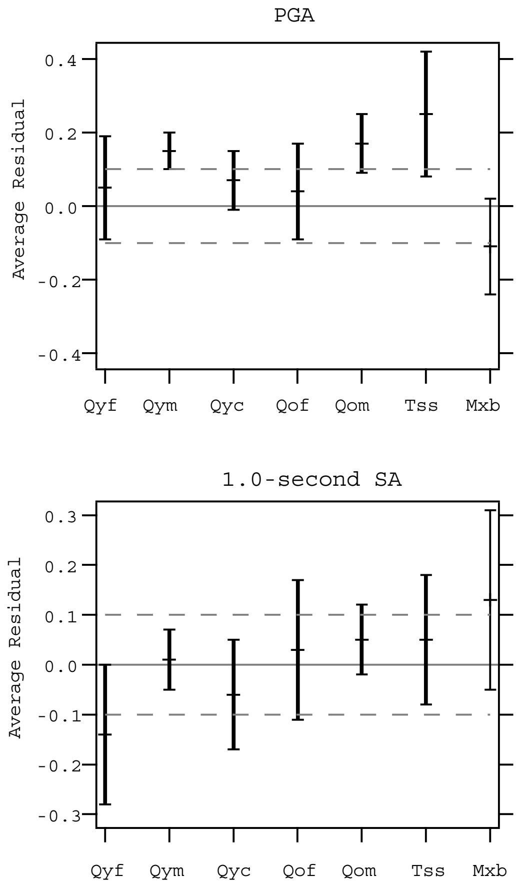

Figure 18. Average residuals (natural log of amplification factor) computed by Lee and Anderson (2000) for the Tinsley and Fumal (1985) detailed-geological units (Fig. 2). The error bars represent plus and minus one standard deviation of the mean.

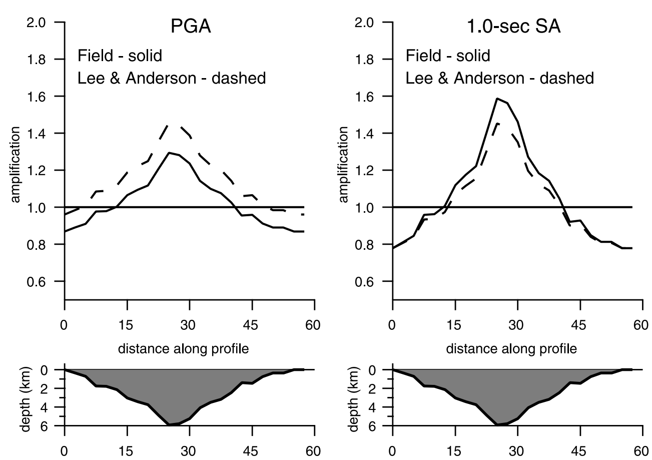

Figure 19. Basin-depth amplification factors implied by the attenuation relationships of Lee and Anderson (2000) and Field (2000), for sites along the first 60 km of the profile shown in Figure 12. The depth profile, chosen specifically to pass near the deepest part of the Los Angeles basin, is shown in cross section below each amplification plot.

and Fumal (1985) map, although more detailed, covers only a relatively small subregion of southern California.

It should be noted that the map provides only an estimate of the actual site category. Site-specific values could differ from mapped categories as a result of any one of the following: (1) errors in the original geological maps; (2) inherent variability of V_{30} that falls outside the defined boundaries; or (3) that the geological unit is less than 30 m in thickness (the "thin alluvium" problem). According to their own statistics, a location on the map has a ~25% chance of being misclassified. Obviously the implications of such errors should be considered carefully in any application.

Field (2000) Attenuation Relationship. In a study closely akin to those of Steidl (2000) and Lee and Anderson (2000), Field (2000) tested whether use of the Wills *et al.* (2000) map is supported by southern California strong-motion data. Because the Boore *et al.* (1997) attenuation relationship is the only one that parameterizes site effects in terms of V_S, it is the natural choice for use with the Wills *et al.* (2000) classification scheme. After determining the Wills *et al.* (2000) site type at each instrument location (Steidl and Lee, 2000), the observations were compared to those predicted by the Boore *et al.* (1997) relationship. Finding some discrepancies, especially for PGA, Field (2000) revised the Boore *et al.* relationship by solving for new parameter coefficients using the southern California data. Coefficients for 3.0-sec SA, which were not provided by Boore *et al.* (1997), were obtained as well.

As shown in Figure 21, Field (2000) found that the five site categories represented in the database (B, BC, C, CD, and D) generally exhibit distinct amplification factors. This is contrary to the conclusions of Steidl (2000) and Lee and Anderson (2000) with respect to the Tinsley and Fumal (1985) map. The one exception is for PGA, where differences do not justify a division into more than two site types (however, one is not led astray by doing so either). The resultant 10%-in-50 yr exceedance values for PGA and 1.0-sec SA are shown in Figure 22 (results for categories A, DE, and E are not shown because they are not represented in the southern California data). The 10%-in-50 yr exceedance levels for 1.0-sec SA are well separated and imply important differences (similar conclusions were obtained with respect to 0.3- and 3.0-sec SA). The differences for PGA are smaller. This latter finding, as discussed by Field (2000) and Field and Petersen (2000), may reflect the influence of sediment nonlinearity in the data.

Like Steidl (2000) and Lee and Anderson (2000), Field (2000) also tested for a basin-depth effect (with depth also defined by the 2.5 km/sec shear-wave isosurface). A significant trend was found for all four ground-motion parameters. The implied amplification factors are included in Figure 19 (solid line) and generally agree with those of Lee and Anderson (2000). For PGA and 1.0-sec SA, respectively, the deepest basin sites have ground motions that are 1.5 and 2.0 times those at the edge. Field (2000) also found that cor-

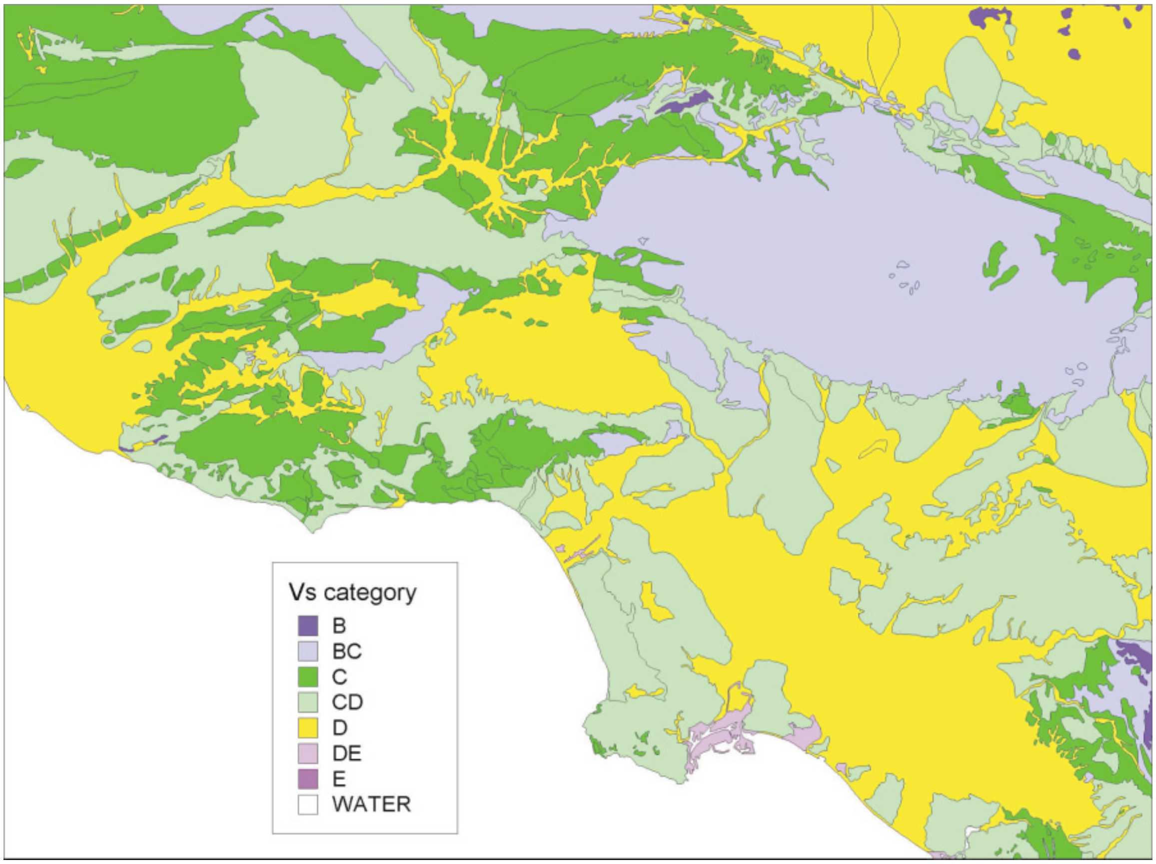

Figure 20. The detailed site classification map of Wills *et al.* (2000), based on the average 30-m shear-wave velocity categories defined in the 1994 NEHRP provisions (Table 2), with 3 intermediate categories added as well (BC, CD, and DE). See Wills *et al.* (2000) for a San Francisco area and a statewide map.

recting for the basin-depth effect did not change sigma significantly. This means the amplification factors can be applied directly to the ground-motion exceedance levels (such as those in Figure 21), without redoing the PSHA calculations.

Note that the basin effect for PGA (up to a 50% amplification) is greater than the 20% difference between site classes D and B in Figure 21. Therefore, it would appear that knowledge of basin depth is more important than V_{30} for PGA. The fact that deep sediments amplify PGA at all, as opposed to deamplify via anelastic attenuation, may seem somewhat surprising. One explanation is that general focusing from the overall basin structure dominates effects of attenuation. Nevertheless, the trend is in qualitative agreement with the 5–7 Hz empirical amplification map of Hartzell *et al.* (1998). The PGA result cannot be an artifact of a correlation between NEHRP category and basin depth, as Field (2000) effectively maximized the influence of the former before inferring the presence of the latter. There remains a possibility, however, that a V_{30} variation within the NEHRP category is correlated with basin depth.

A potential problem with the Field (2000) relationship is that, like Boore *et al.* (1997), sediment nonlinearity is not accounted for in terms of having amplification factors that depend on the ground-motion level. However, as discussed by Field (2000), because sediment sites dominate the database (Steidl and Lee, 2000), nonlinearity may effectively be accounted for in the magnitude, distance, and/or fictitious depth terms. If this were the case, we would expect to see an underprediction of rock-site PGAs at higher ground-motion levels. Unfortunately, there are not enough recordings on rock to adequately test this possibility (Field, 2000). Again, the important question is the accuracy of the model at the magnitudes and distances that dominate hazard ($M \geq$ 6.75 events within 20 km). If the lack of explicit nonlinearity is a problem, it most likely manifests itself as an underprediction of rock-site PGA at high ground-motion levels.

Joyner (2000) Basin Effect. The article by Joyner (2000) presents an alternative perspective on the basin-depth effect. Specifically, he argues that for long-period surface waves, backazimuth distance from the basin edge is the controlling factor (rather than basin depth). The idea, illustrated in Figure 23, is that geometrical spreading is effectively reduced by lateral focusing along the basin edge. Because distance from the edge is generally correlated with basin depth, the

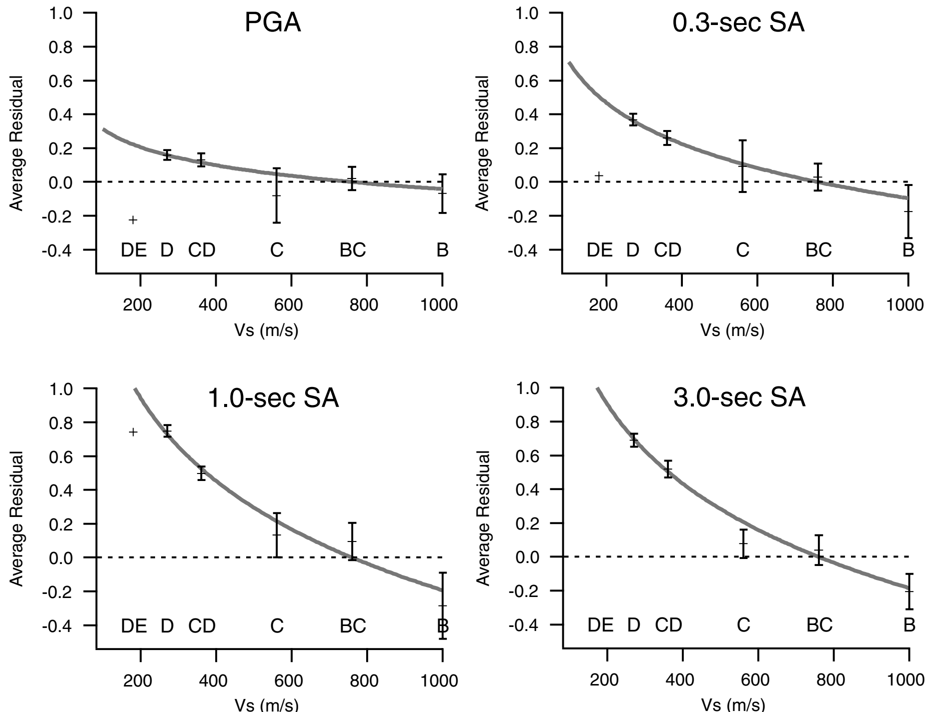

Figure 21. Natural log of amplification factors implied by the Field (2000) attenuation relationship using the Wills *et al.* (2000) classification scheme. The vertical lines represent the average (and plus and minus one standard deviation of the mean) of residuals observed in the southern California database. The solid gray line is the residual predicted by the attenuation relationship. The 30-m velocity assigned to each site category is as follows: D, 270 m/sec; CD, 360 m/sec; C, 560 m/sec; BC, 760 m/sec; and B, 1000 m/sec. The residuals are plotted relative to that predicted for site class BC.

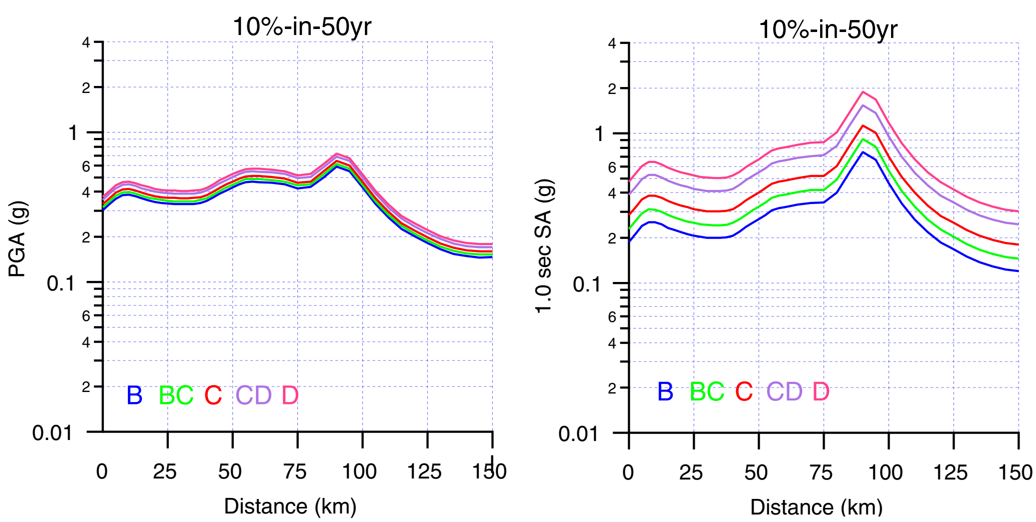

Figure 22. 10%-in-50 yr exceedance values for PGA and 1.0-sec SA predicted by the Field (2000) attenuation relationship for the profile of sites in Figure 12, and using the Wills *et al.* (2000) classification scheme. These exceedance levels do not include the basin-depth effect.

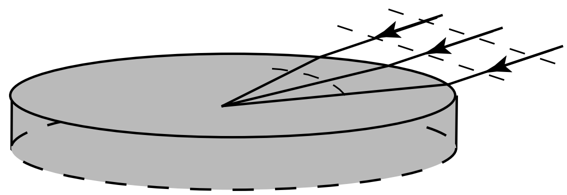

Figure 23. Illustration of Joyner's (2000) notion that the backazimuth distance from the basin edge, rather than depth, is the important factor controlling implied basin amplification.

latter may be a proxy for the former. He provides a model based on regression analysis of long-period ($T \geq 3$ sec) data, which implies amplifications of up to a factor of 3.

Applying this model in PSHA would require tracking the backazimuth distance from basin edge for each earthquake/site pair. A model based on basin depth is obviously much less numerically cumbersome. If Joyner's hypothesis is correct, the relevant question is whether applying the basin-depth correction as a proxy will lead us astray. For example, what happens at the far side of a basin? Under the basin-depth model the amplification comes back down, but with Joyner's model, amplification continues to increase. Interestingly, the 3D simulations of Olsen (2000) shown in Figure 9 suggest the latter. For example, the largest amplification for the San Andreas earthquake (with rupture initiating from the NW) is on the far side of the Los Angeles basin (as opposed to the center). This result implies that the basin-depth effect identified by others may indeed be a proxy for distance from the edge where the waves enter the basin.

Discussion

The complexity in earthquake ground motion resulting from basin effects and scattering in general, coupled with the wide range of size scales of sedimentary deposits, make any definition of site-response ultimately arbitrary. It is therefore important that any site-effect correction be defined and applied in the context of the source- and path-effect model. For PSHA, the most useful definition of site response is in terms of the average behavior, relative to other sites, given all events considered in the analysis. As such, there will likely be a large intrinsic variability with respect to source location.

The maps of Hartzell *et al.* (1998) represent the state of the art in terms of empirical, site-specific amplification factors. However, questions remain whether present data are adequate for such estimates to represent the average for all possible events, especially in light of the results of Wald and Mori (2000). A more justifiable approach, for now at least, is in terms of site-type, rather than site-specific, estimates.

Variability (Epistemic Uncertainty) of PSHA Predictions

Between previously published attenuation relationships and those developed in the Phase III collection of articles we have several viable site-effect parameterizations for southern California. Among all attenuation relationships evaluated by Field and Petersen (2000), the range of 10%-in-50 yr exceedance values implied by each is shown in Figure 24 (where the site type appropriate to each location has been applied). The attenuation relationship associated with each line is not indicated, intentionally, as the point here is to show the variability among all viable estimates. Predicted values in Figure 24 differ by up to a factor of three.

Assuming the source model is reasonably correct, the 10%-in-50 yr exceedance levels for sites considered here are generally dominated by $M \geq 6.75$ earthquakes within ~20 km. Because data are very limited under these conditions (e.g., Figure 15 shows only three such observations for southern California), we can neither say which attenuation relationship is best, nor can we rule out any particular relationship. For this reason, all lines in Figure 24 represent viable estimates of the true 10%-in-50 yr exceedance level, and the variability among predictions represents an estimate of the epistemic uncertainty. That is, time will eventually reveal which, if any, is correct.

Although none of the attenuation relationships can be ruled out, each undoubtedly has its strengths and weaknesses. For example, and as discussed earlier, the Boore *et al.* (1997) model has the disadvantage of not explicitly accounting for nonlinearity and lacking a magnitude-dependent distance decay (Anderson, 2000). Nevertheless, it performs as well as the others in terms of predicting southern California strong-motion data (Lee *et al.,* 2000). It also has the advantage of parameterizing the site-conditions with a continuous variable (V_{30}) rather than with just two or three discrete site types, as in other relationships. For such reasons, experts will likely disagree on which model is best in any given situation. It is even possible that all models are biased at the magnitudes and distances that dominate the hazard.

Detailed Site Classifications

In spite of our inability to choose a preferred attenuation relationship, there are several notable findings with respect to accounting for site effects. For example, Field (2000) has found that corrections based on the site-classification map of Wills *et al.* (2000) are both justified statistically and important in terms of implied ground-motion levels (the exception being PGA, which shows only two distinct categories). This is opposite to the conclusions of Steidl (2000) and Lee and Anderson (2000) with respect to the detailed geology map of Tinsley and Fumal (1985). It would appear that either the latter map is overly detailed, in the sense that amplification factors for the different units are not unique, or that there is not yet enough strong-motion data to reveal its superiority (detailed geology is known for only a subset of observation sites). That the Wills *et al.* (2000) map covers all of California and is based on the 1994 NEHRP categories used in present building codes, is an advantage. However, as with any map, one should be aware of its limitations. For example, they estimate that site-specific V_{30} values have a

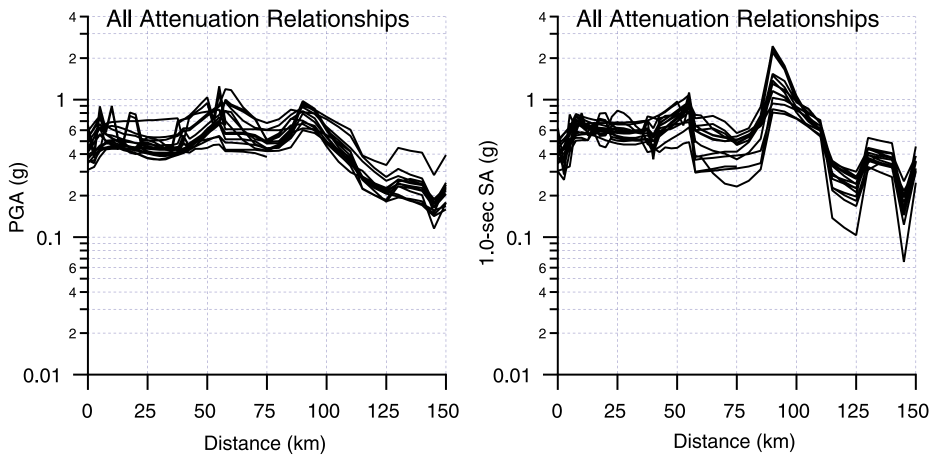

Figure 24. The 10%-in-50 yr exceedance levels across the profile of sites for all the different attenuation relationships evaluated by Field and Petersen (2000), where the site condition specific to each location has been applied. See Figure 10 of Field and Petersen (2000) for more details.

~25% chance of falling outside the range defined for the mapped unit.

Petersen *et al.* (1999) have already used the Wills *et al.* (2000) map, in conjunction with the Boore *et al.* (1997) attenuation relationship, to obtain site-specific hazard maps for the entire state of California. The 10%-in-50 yr exceedance levels obtained using this approach for the first half of the profile of sites are shown in Figure 25 (green line). Note that the site category specific to each location has been applied rather than using uniform site conditions across the entire profile. The evaluation and customization of the Boore *et al.* (1997) attenuation relationship, performed by Field (2000) with respect to southern California data, generally supports the Petersen *et al.* (1999) maps (ignoring the basin depth effect discussed subsequently). The exception is with respect to PGA, where the model of Field (2000) implies less of a difference between type B and type D sites than in the Boore *et al.* (1997) relationship.

Also shown for comparison in Figure 25 are the "firm rock" 10%-in-50 yr values (black line) reflected in the 1996 CDMG/USGS hazard maps (Petersen *et al.,* 1996; Frankel *et al.,* 1996). These latter values are close to, but not exactly the same as those applied in the 1997 NEHRP building code provisions (BSSC, 1998; Leyendecker *et al.,* 2000). The effect of applying the NEHRP amplification factors (Tables 2 and 3) to the rock-site exceedance levels, as specified in the code, is also plotted in Figure 25 (blue line). The results are surprisingly close to the Petersen *et al.* (1999) exceedance levels.

Basin-Depth Effect

Another important finding is the basin-depth effect (Fig. 19). Figure 25 includes the 10%-in-50 yr exceedance levels implied by the Field (2000) attenuation relationship using both the Wills *et al.* (2000) classification and the basin-depth correction (red line). This model implies that for all ground-motion parameters, the deepest basin sites along the profile have the greatest ground-motion levels. This is in contrast to all the other estimates in Figure 25, which imply the greatest level is at the northeast edge of the basin. The difference between the 10%-in-50 yr exceedance estimates of Field (2000) and those obtained with the other site-effect models ranges up to a factor of ~2.4. Interestingly, this manifests more as a reduction along the edge than an increase at the deepest basin sites, which is entirely true for 3.0-sec SA.

The basin-depth effect has been recognized in the context of attenuation relationships previously (e.g., Trifunac and Lee, 1978; Campbell, 1997). With the Phase III studies (Field, 2000; Lee and Anderson, 2000; Steidl, 2000) and including the long-period 3D finite-difference scenario simulations of Olsen (2000), we have a large body of evidence in support of a basin-depth effect. However, the fact that PGA is influenced by basin structure as well is apparently unique to the Phase III studies (Field, 2000; Lee and Anderson, 2000; Steidl, 2000). The model of Field (2000) implies that basin depth has a greater influence on PGA than surface geology (20% versus 50% amplification, respectively). This is somewhat surprising in that we might expect PGA to be reduced, via anelastic attenuation, rather than amplified at deeper basin sites. Perhaps general focusing from basin concavity dominates the influence of anelasticity.

The physical mechanism for the basin effect is not yet clear, as depth may be a proxy for something else. In fact, the actual physical attribute may differ between longer and shorter period ground motion. For example, Joyner (2000) argues that the backazimuth distance from the basin edge, which generally correlates with depth, is the relevant parameter at long periods. If true, applying the correction will be much more numerically cumbersome because the basin-edge distance will have to be computed separately for each earthquake scenario. Therefore, the relevant question seems to be if basin depth is a proxy for something else, will applying it

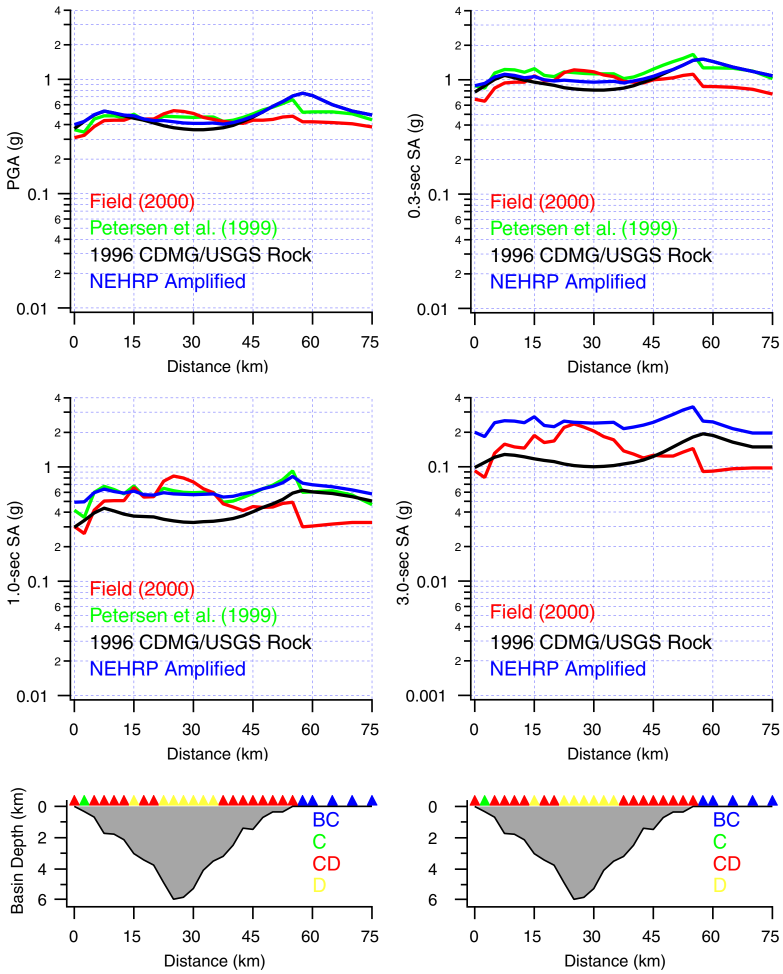

Figure 25. Comparison of 10%-in-50 yr exceedance levels from (1) The 1996 CDMG/USGS hazard maps for rock-site conditions (Petersen *et al.,* 1996; Frankel *et al.,* 1996); (2) The 1996 CDMG/USGS rock-site values multiplied by the NEHRP amplification factors listed in Table 2 (PGA and 0.3-sec SA) and Table 3 (1.0- and 3.0-sec SA), where linear interpolation was applied as necessary. (3) The maps of Petersen *et al.* (1999), where the Boore *et al.* (1997) relationship was applied with the Wills *et al.* (2000) site-classification map (no values are available for 3.0-sec SA); and (4) the values obtained by applying the Field (2000) relationship with both the Wills *et al.* (2000) site-classification and the basin-depth correction. Note that the specific site type at each location is applied (color-coded triangles), and that no B sites are represented along the profile. The plot only extends over the distance range where basin-depth was known.

produce misleading results, or will it be reliable enough for the purposes of PSHA? If Joyner's (2000) hypothesis is correct, the biggest discrepancies will most likely occur at the far sides of basins.

As discussed by Field and Petersen (2000), a comparison of the basin-depth amplification implied by the Phase III studies with that in previous publications (e.g., Trifunac and Lee, 1978; Campbell, 1997) is complicated by differences in depth definitions. This underscores the need to have a consistent, carefully defined, and widely available definition of basin depth. The 2.5 km/sec shear-wave velocity isosurface in the 3D model of Magistrale *et al.* (2000) provides one such standard.

All of the models that have a basin-depth term predict increased shaking above the deepest parts of the basin. This may cause some confusion in that basin edges are known to amplify ground motion via focusing effects. As exemplified previously in Figure 4, the subsurface basin-edge structure near Santa Monica, California, caused large pockets of amplification during the 1994 Northridge earthquake (Gao *et al.,* 1995). However, the very same subsurface structure may have defocused energy at adjacent sites (Alex and Olsen, 1998). Recall that with respect to PSHA, we are interested in the amplification pattern averaged over all earthquakes of concern. For this, it appears that amplitudes are greater for sites farther from the edge. However, we might expect ground motion to be intrinsically more variable (i.e., larger sigma) near the edges.

Influence of Prediction Error (Sigma)

For the southern California sites examined, Field and Petersen (2000) demonstrated that changing the attenuation-relationship prediction error (sigma) by more than $\sim$0.1, in natural log units, produces a greater than 10% change in the 10%-in-50 yr exceedance level. As implied by differences between originally published sigma values and those calculated by Lee *et al.* (2000) with southern California data, epistemic uncertainties of sigma may well exceed this amount, especially at the magnitudes and distances dominating the hazard. Therefore, further refinements in our understanding of sigma, including the degree of magnitude dependence, will likely have an important impact on seismic hazard estimates.

All Phase-III attenuation-relationship studies (Field, 2000; Lee and Anderson, 2000; Steidl, 2000) concluded that the detailed-site and/or basin-depth corrections produce only a small reduction in sigma. None of the models invokes a change in sigma for the detailed-site or basin-depth corrections. This inspired Lee and Anderson (2000) to apply the residual versus residual analysis of Lee *et al.* (1998), which provides an estimate of the maximum amount sigma can be reduced by accounting for site effects, without the requirement of knowing what the site corrections are. Their results support the contention that site-effect corrections, at least in southern California, cannot be relied upon to make important reductions in sigma. In other words, the intrinsic variability caused by basin-edge-induced surface waves, focusing and defocusing effects, and scattering in general, create an intrinsic variability that cannot be reduced in any model that quantifies ground motion with so few parameters.

It is possible that some part of sigma comes from a misclassification of site types in the database. For example, Wills *et al.* (2000) estimate a ~25% chance of misclassification with respect to their site-effect map. In effect, these errors have been folded into the prediction error (sigma) of the Field (2000) attenuation relationship. However, it seems doubtful that such misclassification makes a relatively strong contribution compared to the intrinsic variability of ground motion caused by scattering.

Caveats

Although all attenuation relationships evaluated in the Phase III studies are viable, that of Field (2000) seems most advantageous in that it incorporates both the detailed site classification of Wills *et al.* (2000) and a basin-depth effect. However, the model does not explicitly account for nonlinear sediment effects, which as discussed by the author, may manifest as an underprediction of rock-site amplitudes at higher levels of shaking.

In addition, all Phase III attenuation relationships assume that the southern California strong-motion database is representative of average, long-term behavior. The hope has been that we have learned something unique about the region (e.g., that basin depth is significant and important; that the detailed geology of Tinsley and Fumal (1985) is not useful). However, we must acknowledge the possibility that database limitations may have led us astray.

Finally, it is important to note that our findings are relevant to dominant magnitudes and distances implied by the hazard model and to the site conditions that typify southern California. For example, NEHRP class E is not present in the area and has, therefore, been ignored. The Wills *et al.* (2000) class DE (V_{30} = 180 m/sec) does exist (e.g., near Long Beach harbor), but strong-motion observations are generally lacking for this category. Understanding the influence of these site types is very important, especially in regions such as the San Francisco Bay area.

Future Research

The large variability (or epistemic uncertainty) in exceedance levels predicted by different attenuation relationships highlights the importance of understanding ground motion under conditions that dominate the hazard (e.g., $M \geq 6.75$ earthquakes at distances less than ~20 km). Also important is the influence of sediment nonlinearity at high ground-motion levels. Because southern California data are presently inadequate to resolve these issues, we must either wait for more observations or include data from other regions.

In their "Proposal for Modifying the Site Coefficients in the NEHRP Provisions," Joyner and Boore (written comm.) have already taken the latter approach of using a broader range of data. Reviewing recent work by themselves and others, they find support for the degree of nonlinearity in the NEHRP F_a amplification factors (Table 2), but find no evidence of nonlinearity for F_v (Table 3). Another remaining question is whether applying the site correction within the hazard calculations, as opposed to after the hazard calculations (as in present building codes), will lead to important differences.

Attenuation relationships are constantly being updated, particularly now given the recent spate of $M \geq 7$ events. These include the Kocaeli earthquake in Turkey (e.g., Toksöz *et al.,* 1999), the Hector Mine earthquake in southern California (e.g., Scientists from the USGS, SCEC, and CDMG, 2000), and the Chi-Chi earthquake in Taiwan (Shin *et al.,* 2000). In addition to providing interim models, the Phase III studies can serve as a guide to authors as they make further refinements to their attenuation relationships. Specifically, a site categorization based both on V_{30} and on a basin-depth parameter seems well supported by data. In fact, for PGA the basin-depth effect seems more important than near-surface conditions. However, additional research is needed to determine whether basin-depth is a proxy for something else (such as distance from the edge, or near-surface variations not accounted for in the models), and whether applying it anyway will lead one astray.

Although some additional refinements will be forthcoming, especially in terms of identifying the true mean and standard deviation of ground motion at the magnitudes and distances dominating hazard, a significant intrinsic (or aleatory) uncertainty will remain. That is, due to basin effects, subsurface focusing, and scattering in general, the prediction uncertainty associated with any model that represents ground motion with only a few parameters will remain high. Of course it is possible that sigma of an attenuation relationship could be reduced appreciably by adding more and more parameters to the model. However, eventually it becomes easier, and certainly more elegant, to model ground motion more explicitly from first principles of physics. In fact, the latter approach is probably our only hope for dramatically reducing the uncertainty of ground-motion predictions. Such waveform modeling is also in line with the trend toward dynamic analysis in the engineering community, as complete seismograms are necessary to compute the full nonlinear response of a structure. However, important uncertainties will likely remain with waveform modeling as well, as ground motion is known to be sensitive to the exact distribution of rupture on a fault. Nevertheless, waveform modeling represents our best hope for making more accurate estimates of ground motion at a site. It will also help constrain attenuation relationships at the larger-magnitude/short-distance conditions that dominate hazard and are underrepresented in the data. The accuracy and maximum frequency of waveform modeling will inevitably increase in the future with more refined structural models and advances in high-performance computing.

Acknowledgments

We thank Susan Hough, Roger Borcherdt, Paul Somerville, and Norman Abrahamson for written reviews of this manuscript. We are especially grateful to Kenneth Campell for timely and comprehensive reviews of this and several of the other Phase III articles as well. Stephen Hartzell and Jack Moehle also commented. Susan Hough's investigative work unearthed the site-effect reference of Drake (1815). This research was supported by the Southern California Earthquake Center (SCEC) and the United States Geological Survey (USGS). SCEC is funded by NSF Cooperative Agreement EAR-8920136 and USGS Cooperative Agreements 14-08-0001-A0899 and 1434-HQ-97AG01718. The SCEC Contribution Number for this article is 535.

References

Abrahamson, N. A., and K. M. Shedlock (1997). Overview, *Seism. Res. Lett.* **68,** 9–23.

Abrahamson, N. A., and W. Silva (1997). Empirical response spectral attenuation relations for shallow crustal earthquakes, *Seism. Res. Lett.* **68,** 94–127.

Aki, K. (1957). Space and time spectra of stationary stochastic waves with special reference to microtremors, *Bull. Earthquake Res. Inst.* **35,** 415–456.

Aki, K. (1988). Local site effects on strong ground motion, in *Proc. Earthquake Engineering and Soil Dynamics II,* Park City, Utah, June 27–30, 103–155.

Aki, K. (1993). Local site effects on weak and strong ground motion, *Tectonophysics* **218,** 93–111.

Aki, K., and B. Chouet (1975). Origin of coda waves: source, attenuation, and scattering effects, *J. Geophys. Res.* **80,** 3322–3342.

Aki, K., and I. Irikura (1991). Characterization and mapping of earthquake shaking for seismic zonation, in *Proc. of the 4th International Conf. on Seismic Zonation,* Stanford, California, Vol. 1, August 25–29, 61–110.

Aki, K., and P. G. Richards (1980). *Quantitative Seismology,* Vol. 1, W. H. Freeman, San Francisco.

Aki, K., G. R. Martin, B. H. Chin, N. Abrahamson, A. C. Cornell, and M. Mahdyiar (1995). Probabilistic seismic hazard analysis and the development of earthquake scenario time histories for southern California sites, TASK H-7 of the Southern California Earthquake Center Report on the Characteristics of Earthquake Ground Motions for Seismic Design.

Alex, C. M., and K. B. Olsen (1998). Lens-Effect in Santa Monica? *Geophys. Res. Lett.* **25,** 3441–3444.

Anderson, J. G. (2000). Expected shape of regressions for ground-motion parameters on rock, *Bull. Seism. Soc. Am.* **90,** no. 6B, S43–S52.

Anderson, J. G., and S. E. Hough (1984). A model for the shape of the Fourier amplitude spectrum of acceleration at high frequencies, *Bull. Seism. Soc. Am.* **74,** 1969–1994.

Anderson, J. G., Y. Lee, Y. Zeng, and S. Day (1996). Control of strong motion by the upper 30 meters, *Bull. Seism. Soc. Am.* **86,** 1749–1759.

Andrews, D. J. (1986). Objective determination of source parameters and similarity of earthquakes of different size, in *Earthquake Source Mechanics,* S. Das, J. Boatwright, and C. H. Scholz (Editors), American Geophysical Union, Washington, D.C., 259–268.

Archuleta, R. J. (1998). Direct observation of nonlinear soil response in acceleration time histories (abstract), *Seism. Res. Lett.* **69,** 148.

Bard, P.-Y. (1994). Effects of surface geology on ground motion: recent results and remaining issues, in *Proc. 10th European Conf. on Earthquake Engineering* **1,** 305–325.

Bard, P.-Y. (1998). Microtremor measurements: a tool for site effect estimation? *Proc. of the 2nd Int. Symp. on Effects of Surface Geology on Seismic Motion,* Yokohama, Japan, 1–3 December, Vol. 3, 1251–1282.

Bazzurro, P., and C. A. Cornell (1999). Disaggregation of Seismic Hazard, *Bull. Seism. Soc. Am.* **89,** 501–520.

Beresnev, I. A., and K.-L. Wen (1996). Nonlinear soil response: a reality? *Bull. Seism. Soc. Am.* **86,** 1964–1978.

Beresnev, I. A., G. M. Atkinson, P. A. Johnson, E. H. Field (1998). Stochastic finite-fault modeling of ground motions from the 1994 Northridge, California earthquake. II widespread nonlinear response at soil sites, *Bull. Seism. Soc. Am.* **88.**

Boore, D. M., W. B. Joyner, and T. E. Fumal (1993). Estimation of response spectra and peak accelerations from western North American earthquakes: an interim report, *U.S. Geol. Surv. Open-File Rept. 93-509,* 72 pp.

Boore, D. M., W. B. Joyner, and T. E. Fumal (1997). Equations for estimating horizontal response spectra and peak acceleration from western North American earthquakes: a summary of recent work, *Seism. Res. Lett.* **68,** 128–153.

Bonilla, L. F., J. H. Steidl, G. T. Lindley, A. G. Tumarkin, and R. J. Archuleta (1997). Site amplification in the San Fernando Valley, California: variability of site-effect estimation, *Bull. Seis. Soc. Am.* **87,** 710–730.

Bonilla, L. F., D. Lavallée, and R. J. Archuleta (1998). Nonlinear site response: Laboratory modeling as a constraint for modeling accelerograms, in *Proc. of the 2nd Int. Symp. on Effects of Surface Geology* on Seismic Motion 2, edited by K. Irikura, K. Kudo H. Okada and T. Sasatani, A. A. Balkema: Netherlands, 793–800.

Borcherdt, R. D. (1970). Effects of local geology on ground motion near San Francisco Bay, *Bull. Seism. Soc. Am.* **60,** 29–61.

Borcherdt, R. D. (1985). Predicting earthquake ground motion: an introduction, *U.S. Geol. Surv. Profess. Pap. 1360,* 93–99.

Borcherdt, R. D. (1993). On the estimation of site-dependent response spectra, in Proc. International Workshop on Strong-Motion Data, Menlo Park, California, Port and Harbor Research Institute, Japan, vol. 2, 399–427.

Borcherdt, R. D. (1994). Estimates of site-dependent response spectra for design (methodology and justification), *Earthquake Spec.* **10,** 617–653.

Borcherdt, R. D. (1996). Preliminary amplification estimates inferred from strong ground motion recordings of the Northridge earthquake of January 17, 1994, in *Proc. of the International Workshop on Site Response Subjected to Strong Ground Motion,* Port and Harbour Research Institute, Yokosuka, Japan, 16–17 January, 1996, Vol. 1.

Borcherdt, R. D., and G. Glassmoyer (1992). On the character of local geology and their influence on ground motions generated by the Loma Prieta earthquake in the San Francisco Bay region, California, *Bull. Seism. Soc. Am.* **82,** 603–641.

Bullen, K. E. (1965). *An Introduction to the Theory of Seismology,* Cambridge University Press, Cambridge.

Building Seismic Safety Council (BSSC) (1995). 1994 Edition NEHRP Recommended Provisions for Seismic Regulations for New Buildings, FEMA 222A/223A, developed for the Federal Emergency Management Agency, Washington, D.C.

Building Seismic Safety Council (BSSC) (1998). 1997 Edition NEHRP Recommended Provisions for Seismic Regulations for New Buildings, FEMA 302/303, developed for the Federal Emergency Management Agency, Washington, D.C.

Campbell, K. W. (1997). Empirical near-source attenuation relationships for horizontal and vertical components of peak ground acceleration, peak ground velocity, and pseudo-absolute acceleration response spectra, *Seism. Res. Lett.* **68,** 154–179.

Chang, S. W., and Bray, J. D. (1997). Implications of recent strong motion data for seismic building code design at deep, stiff soil sites, Proc. CUREe Northridge Earthquake Research Conference, Los Angeles, California.

Chin, B.-H., and K. Aki (1996). Reply to "Comment on Simultaneous study of the source, path, and site effects on strong ground motion during the Loma Prieta earthquake: a preliminary result on pervasive nonlinear effects" by L. Wennerberg, *Bull. Seism. Soc. Am.* **86,** 268–273.

Cornell, A. (1968). Engineering seismic risk analysis, *Bull. Seism. Soc. Am.* **58,** 1583–1606.

Cramer, C. H., and M. D. Petersen (1996). Predominant seismic source distance and magnitude maps for Los Angeles, Orange, and Ventura counties, California, *Bull. Seism. Soc. Am.* **86,** 1645–1649.

Day, S. M. (1996). RMS response of a one-dimensional halfspace to SH, *Bull. Seism. Soc. Am.* **86,** 363–370.

Dobry, R., R. D. Borcherdt, C. B. Crouse, I. M. Idriss, W. B. Joyner, G. R. Martin, M. S. Power, E. E. Rinne, and R. B. Seed (2000). New site coefficients and site classification system used in recent building seismic code provisions, *Earthquake Spectra* **16,** 41–68.

Drake, D. (1815). *Natural and Statistical View, or Picture of Cincinnati and the Miami County, Illustrated by Maps,* Looker and Wallace, Cincinnati.

Field, E. H. (1996). Spectral amplification in a sediment-filled valley exhibiting clear basin-edge induced waves, *Bull. Seism. Soc. Am.* **86,** 991–1005.

Field, E. H. (2000). A modified ground-motion attenuation relationship for southern California that accounts for detailed site classification and a basin-depth effect, *Bull. Seism. Soc. Am.* **90,** no. 6B, S209–S221.

Field, E. H., and S. E. Hough (1996). The Variability of PSV Response Spectra Across a Dense Array Deployed During the Northridge Aftershock Sequence, *Earthquake Spectra,* **13,** 243–257.

Field, E. H., and M. D. Petersen (2000). A test of various site-effect parameterizations in probabilistic seismic hazard analyses of southern California, *Bull. Seism. Soc. Am.* **90,** no. 6B, S222–S244.

Field, E. H., P. A. Johnson, I. A. Beresnev, and Y. Zeng (1997). Nonlinear ground-motion amplification by sediment during the 1994 Northridge earthquake, *Nature* **390,** 599–602.

Field, E. H., S. Kramer, A.-W. Elgamal, J. D. Bray, N. Matasovic, P. A. Johnson, C. Cramer, C. Roblee, D. J. Wald, L. F. Bonilla, P. P. Dimitriu, and J. G. Anderson (1998a). Nonlinear site response: where we're at (a report from a SCEC/PEER seminar and workshop), *Seism. Res. Lett.* **69,** 230–234.

Field, E. H., Y. Zeng, P. A. Johnson, and I. A. Beresnev (1998b). Pervasive nonlinear sediment response during the 1994 Northridge earthquake: observations and finite-source simulations, *J. Geophys. Res.* **103,** 26869–26883.

Field, E. H., D. D. Jackson, and J. F. Dolan (1999). A mutually consistent seismic-hazard source model for southern California, *Bull. Seism. Soc. Am.* **89,** 559–578.

Frankel, A. (1993). Three-dimensional simulations of ground motions in the San Bernardino Valley, California, for hypothetical earthquakes on the San Andreas fault, *Bull. Seism. Soc. Am.* **83,** 1020–1041.

Frankel, A. (1994). Dense array recordings in the San Bernardino Valley of Landers-Big Bear aftershocks: basin surface waves, Moho reflections, and three-dimensional simulations, *Bull. Seism. Soc. Am.* **84,** 613–624.

Frankel, A., C. Mueller, T. Barnhard, D. Perkins, E. V. Leyendecker, N. Dickman, S. Hanson, and M. Hopper (1996). National seismic-hazard maps: documentation, *U.S. Geol. Surv. Open-File Rept. 96-352.*

Fumal, T. E., and J. C. Tinsley (1985). Mapping shear-wave velocities of near-surface geologic materials, *U.S. Geol. Surv. Profess. Pap. 1360,* 127–150.

Gao, S., H. Liu, P. M. Davis, and L. Knopoff (1996). Localized amplification of seismic waves and correlation with damage due to the Northridge earthquake, *Bull. Seism. Soc. Am.* **85,** S209–S230.

Graves, R. W., A. Pitarka, and P. G. Somerville (1998). Ground motion amplification in the Santa Monica area: effects of shallow basin edge structure, *Bull. Seism. Soc. Am.* **88,** 1224–1242.

Gutenberg, B. (1957). Effects of ground on earthquake motion, *Bull. Seism. Soc. Am.* **47,** 221–250.

Hanks, T. C. (1975). Strong ground motion of the San Fernando, California, earthquake: ground displacements, *Bull. Seism. Soc. Am.* **65,** 193–225.

Harmsen, S. C. (1997). Determination of site amplification in the Los Angeles urban area from inversion of strong-motion records, *Bull. Seism. Soc. Am.* **87,** 866–887.

Hartzell, S. (1998). Variability in nonlinear sediment response during the 1994 Northridge, California, earthquake, *Bull. Seism. Soc. Am.* **88,** 1426–1437.

Hartzell, S., A. Leeds, A. Frankel, and J. Michael (1996). Site response for urban Los Angeles using aftershocks of the Northridge Earthquake, *Bull. Seism. Soc. Am.* **86,** S168–S192.

Hartzell, S., E. Cranswick, A. Frankel, D. Carver, and M. Meremonte (1997). Variability of site response in the Los Angeles urban area, *Bull. Seism. Soc. Am.* **87,** 1377–1400.

Hartzell, S., S. Harmsen, A. Frankel, D. Carver, E. Cranswick, M. Meremonte, and J. Michael (1998). First generation site-response maps for the Los Angeles region based on earthquake ground motions, *Bull. Seism. Soc. Am.* **88,** 463–472.

Haskell, N. A. (1960). Crustal reflection of plane SH waves, *J. Geophys. Res.* **65,** 4147–4150.

Hough, S. E., C. Dietel, G. Glassmoyer, and E. Sembera (1995). On the variability of aftershock ground motion in the San Fernando Valley, *Geophys. Res. Lett.* **22,** 727–730.

Hudson, D. E. (1972). Local distribution of strong earthquake ground motions, *Bull. Seism. Soc. Am.* **62,** 1765–1786.

Idriss, I. M., and H. B. Seed (1968). Seismic response of horizontal layers, *Proc. Am. Soc. Civil Eng. J. Soil Mech. Found. Div.* **94,** 1003–1031.

Joyner, W. B., R. E. Warrick, and T. E. Fumal (1981). The effect of Quaternary alluvium on strong ground motion in the Coyote Late, California, earthquake of 1979, *Bull. Seism. Soc. Am.* **71,** 1333–1349.

Joyner, W. B., and T. E. Fumal (1985). Predictive mapping of earthquake ground motion, *U.S. Geol. Surv. Profess. Pap. 1360,* 203–220.

Joyner, W. B. (2000). Strong motion from surface waves in deep sedimentary basins, *Bull. Seism. Soc. Am.* **90,** no. 6B, S95–S112.

Kagami, H., C. M. Duke, G. C. Liang, and Y. Ohta (1982). Observation of 1- to 5-second microtremors and their application to earthquake engineering. II. Evaluation of site effect upon seismic wave amplification due to extremely deep soils, *Bull. Seism. Soc. Am.* **72,** 987–998.

Kagami, H., S. Okada, K. Shiono, M. Oner, M. Dravinski, and A. K. Mal (1986). Observation of 1- to 5-second microtremors and their application to earthquake engineering. III. A two-dimensional study of site effects in the San Fernando Valley, *Bull. Seism. Soc. Am.* **76,** 1801–1812.

Kato, K., K. Aki, and M. Takemura (1995). Site amplification from Coda Waves: validation and application to *S*-wave site response, *Bull. Seism. Soc. Am.* **85,** 467–477.

Lee, Y., and J. G. Anderson (2000). Potential for improving ground-motion relations in southern California by incorporating various site parameters, *Bull. Seism. Soc. Am.* **90,** no. 6B, S170–S186.

Lee, Y., Y. Zeng, and J. G. Anderson (1998). A simple strategy to examine the sources of errors in attenuation relations, *Bull. Seism. Soc. Am.* **88,** 291–296.

Lee, Y., J. G. Anderson, and Y. Zeng (2000). Evaluation of empirical ground-motion relations in southern California, *Bull. Seism. Soc. Am.* **90,** no. 6B, S136–S148.

Leyendecker, E. V., R. J. Hunt, A. D. Frankel, and K. S. Rukstales (2000). Development of maximum considered earthquake ground motion maps, *Spectra* **16,** 21–40.

Liu, H.-L., and T. H. Heaton (1984). Array analysis of the ground velocities and accelerations from the 1971 San Fernando, California, earthquake, *Bull. Seism. Soc. Am.* **74,** 1951–1968.

Magistrale, H., S. Day, R. W. Clayton, and R. Graves (2000). The SCEC southern California reference three-dimensional seismic velocity model version 2, *Bull. Seism. Soc. Am.* **90,** no. 6B, S65–S76.

Margheriti, L., L. Wennerberg, and J. Boatwright (1994). A comparison of coda and S-wave spectral ratios as estimates of site response in the southern San Francisco Bay area, *Bull. Seism. Soc. Am.* **84,** 1815–1830.

McGuire, R. K. (1995). Probabilistic seismic hazard analysis and design earthquakes; closing the loop, *Bull. Seism. Soc. Am.* **85,** 1275–1284.

McGuire, R. K., and K. M. Shedlock (1981). Statistical uncertainties in seismic hazard evaluations in the United States, *Bull. Seism. Soc. Am.* **71,** 1287–1308.

Meremonte, M., A. Frankel, E. Cranswick, D. Carver, and D. Worley (1996). Urban seismology: Northridge aftershocks recorded by multiscale arrays of portable digital seismographs, *Bull. Seism. Soc. Am.* **86,** 1350–1363.

Milne, J. (1898). *Seismology,* first Ed., Kegan Paul, Trench, Trube, London.

Navaro, O., T. H. Seligman, J. M. Alvarez-Tostado, J. L. Mateos, and J. Flores (1990). Two-dimensional model for site-effect studies of microtremors in the San Fernando Valley, *Bull. Seism. Soc. Am.* **80,** 239–251.

Ni, S.-D., J. G. Anderson, Y. Zeng, and R. V. Siddharthan (2000). Expected signature of nonlinearity on regression for strong ground-motion parameters, *Bull. Seism. Soc. Am.* **90,** no. 6B, S53–S64.

O'Connell, D. R. H. (1999). Replication of apparent nonlinear seismic response with linear wave propagation models, *Science* **283,** 2045–2050.

Okada, H. T., S. Matsushima, and E. Hidaka (1987). Comparison of spatial autocorrelation method and frequency-wave number spectral method of estimating the phase velocity of Rayleigh waves in long-period microtremors, *Geophys. Bull. Hokkaido Univ.* **49,** 53–62.

Olsen, K. B. (2000). Site amplification in the Los Angeles basin from three-dimensional modeling of ground motion, *Bull. Seism. Soc. Am.* **90,** no. 6B, S77–S94.

Park, S., and S. Elrick (1998). Predictions of shear-wave velocities in southern California using surface geology, *Bull. Seism. Soc. Am.* **88,** 677–685.

Petersen, M. D., W. A. Bryant, C. H. Cramer, T. Cao, Michael S. Reichle, A. D. Frankel, J. J. Lienkaemper, P. A. McCrory and D. P. Schwartz (1996). Probabilistic seismic hazard assessment for the State of California, *Calif. Div. Mines Geol. Open-File Rept. 96-08; U.S. Geol Surv Open-File Rept. 97-706,* 33 pp.

Petersen, M., D. Beeby, W. Bryant, C. Cao, C. Cramer, J. Davis, M. Reichle, G. Saucedo, S. Tan, G. Taylor, T. Toppozada, J. Treiman, and C. Wills (1999). Seismic shaking hazard maps of California, *Calif. Div. Mines Geol. Map Sheet 48.*

Petersen, M. D., C. H. Cramer, M. S. Reichle, A. D. Frankel, and T. C. Hanks (2000). Discrepancy between earthquake rates implied by historic earthquakes and a consensus geologic source model for California, *Bull. Seism. Soc. Am.* **90,** 1117–1132.

Phillips, W. S., and K. Aki (1986). Site amplification of coda waves from local earthquakes in central California, *Bull. Seism. Soc. Am.* **76,** 627–648.

Reid, H. F. (1910). The California earthquake of April 18, 1906: report of the state earthquake investigation commission, Carnegie Institute, Washington, D.C., Publ. 87, Vol. 2.

Reiter, L. (1990). *Earthquake Hazard Analysis: Issues and Insights,* Columbia University Press, New York, 254 pp.

Rogers, A. M., J. C. Tinsley, W. W. Hays, and K. W. King (1979). Evaluation of the relation between near-surface geologic units and ground response in the vicinity of Long Beach, California, *Bull. Seism. Soc. Am.* **61,** 1603–1622.

Rogers, A. M., R. D. Borcherdt, P. A. Covington, and D. M. Perkins (1984). A comparative ground response study near Los Angeles using recordings of Nevada nuclear tests and the 1971 San Fernando earthquake, *Bull. Seism. Soc. Am.* **74,** 1925–1949.

Rogers, A. M., J. C. Tinsley, and R. D. Borcherdt (1985). Predicting relative ground response, *U.S. Geol. Surv. Profess. Pap. 1360,* 221–248.

Sadigh, K., C. Y. Chang, J. A. Egan, F. Makdisi, and R. R. Youngs (1997). Attenuation relationships for shallow crustal earthquakes based on California strong motion data, *Seism. Res. Lett.* **68,** 180–189.

Scientists from the USGS, SCEC, and CDMG (2000). Preliminary report on the 16 October 1999 M 7.1 Hector Mine, California, earthquake, *Seism. Res. Lett.* **71,** 11–23.

Schnabel, P., H. B. Seed, and J. Lysmer (1972). Modification of seismograph records for effects of local soil conditions, *Bull. Seism. Soc. Am.* **62,** 1649–1664.

Scrivner, C. W., and D. Helmberger (1999). Variability of ground motions in southern California: data from the 1995 and 1996 Ridgecrest sequence, *Bull. Seism. Soc. Am.* **89,** 626–639.

Seekins, L. C., L. Wennerberg, L. Margheriti, and H.-P. Liu (1996). Site amplification at five locations in San Francisco: a comparison of *S*-waves, codas, and microtremors, *Bull. Seism. Soc. Am.* **86,** 627–635.

Senior Seismic Hazard Analysis Committee (SSHAC) (1997). Recommendations for probabilistic seismic hazard analysis: guidance on uncertainty and use of experts, U.S. Nuclear Regulatory Commission, U.S. Dept. of Energy, Electric Power Research Institute; NUREG/CR-6372, UCRL-ID-122160, Vol. 1–2. Also a review of the document by National Academy Press, Washington, D.C., 73 pp.

Shin, T. C., K. W. Kuo, W. H. K. Lee, T. L. Teng, and Y. B. Tsai, 2000). A preliminary report on the 1999 Chi-Chi (Taiwan) earthquake, *Seism. Res. Lett.* **71,** 24–30.

Spudich, P. A., and S. H. Hartzell (1985). Predicting earthquake ground-motion time-histories, *U.S. Geol. Surv. Profess. Pap. 1360,* 221–247.

Spudich, P. A. (1997). What seismology may be able to bring to future building codes, Presented at ATC-35 Ground Motion Initiative Workshop, Rancho Bernardino, California 30–31 July 1997.

Steidl, J. H. (1993). Variation of Site Response at the UCSB Dense Array of Portable Accelerometers, *Earthquake Spectra* **9,** 289–302.

Steidl, J. H. (2000). Site response in southern California for probabilistic seismic hazard analysis, *Bull. Seism. Soc. Am.* **90,** no. 6B, S149–S169.

Steidl, J. H., and Y. Lee (2000). The SCEC Phase III strong-motion database, *Bull. Seism. Soc. Am.* **90,** no. 6B, S113–S135.

Su, F., and K. Aki (1995). Site amplification factors in central and southern California determined from coda waves, *Bull. Seism. Soc. Am.* **85,** 452–466.

Su, F., J. G. Anderson, and Y. Zeng (1998). Study of weak and strong ground motion including nonlinearity from the Northridge, California earthquake sequence, *Bull. Seism. Soc. Am.* **88,** 1411–1425.

Tinsley, J. C., and T. E. Fumal (1985). Mapping Quaternary sedimentary deposits for areal variations in shaking response, *U.S. Geol. Surv. Profess. Pap. 1360,* 101–126.

Toksöz, M. N., R. E. Reilinger, C. G. Doll, A. A. Barka, and N. Yalcin (1999). Izmit (Turkey) earthquake of 17 August 1999: first report, *Seism. Res. Lett.* **70,** 669–679.

Toro, R. G., N. A. Abrahamson, and J. F. Schneider (1997). Model of strong ground motions from earthquakes in central and eastern North America: best estimates and uncertainties, *Seism. Res. Lett.* **68,** 41–57.

Tsujiura, M. (1978). Spectral analysis of coda waves from local earthquakes, *Bull. Earthquake Res. Inst. Tokyo Univ.* **53,** 1–48.

Trifunac, M. D., and V. W. Lee (1978). Dependence of the Fourier amplitude spectra of strong motion acceleration on the depth of sedimentary deposits, University of Southern California, Department of Civil Engineering, Report No. CE 78-14, Los Angeles.

U.S. Geological Survey (USGS) (1985). Evaluating earthquake hazard in the Los Angeles region, *U.S. Geol. Surv. Profess. Pap. 1360.*

Vidale, J. E., and D. V. Helmberger (1988). Elastic finite-difference modeling of the 1971 San Fernando, California earthquake, *Bull. Seism. Soc. Am.* **78,** 122–141.

Wald, D. J., and R. W. Graves (1998). The seismic response of the Los Angeles Basin, California, *Bull. Seism. Soc. Am.* **88,** 337–356.

Wald, L. A., and J. Mori (2000). Evaluation of methods for estimating linear site-response amplifications in the Los Angeles region, *Bull. Seism. Soc. Am.* **90,** no. 6B, S32–S42.

Wennerberg, L. (1996). Comment on "Simultaneous study of the source, path, and site effects on strong ground motion during the Loma Prieta earthquake: a preliminary result on pervasive nonlinear effects" by B.-H Chin and K. Aki, *Bull. Seism. Soc. Am.* **86,** 259–267.

Wills, C. J., M. Petersen, W. A. Bryant, M. Reichle, G. J. Saucedo, S. Tan, G. Taylor, and J. Treiman (2000). A site-conditions map for California based on geology and shear-wave velocity, *Bull. Seism. Soc. Am.* **90,** no. 6B, S187–S208.

Wood, H. D. (1908). Distribution of apparent intensity in San Francisco, in the California earthquake of April 18, 1906, report of the State Earthquake Investigation Commission, Carnegie Institute, Washington, D.C., Publ. 87, 220–245.

Wood, H. D. (1933). Preliminary report on the Long Beach earthquake, *Bull. Seism. Soc. Am.* **23,** 42–56.

Working Group on California Earthquake Probabilities (WGCEP) (1995). Seismic hazards in southern California: probable earthquakes, 1994 to 2024. *Bull. Seism. Soc. Am.* **85,** 379–439.

Working Group on California Earthquake Probabilities (WGCEP) (1999). Earthquake probabilities in the San Francisco Bay region: 2000 to 2030: a summary of findings, *U.S. Geol. Surv. Open-File Rept. 99-517.*

Yamanaka, H., M. Dravinski, and H. Kagami (1993). Continuous measurements of microtremors on sediments and basement in Los Angeles, California, *Bull. Seism. Soc. Am.* **83,** 1595–1609.

Yamanaka, H., M. Takemura, H. Ishida, and M. Niwa (1994). Characteristics of long-period microtremors and their applicability in exploration of deep sedimentary layers, *Bull. Seism. Soc. Am.* **84,** 1831–1841.

Yoshida, N., and S. Iai (1998). Nonlinear site response and its evaluation and prediction, in *Proc. Second Int. Symp. on Effects of Surface Geology on Seismic Motion,* Yokohama, Japan, 1–3 December, Vol. 1, 71–90.

Yu, G., J. G. Anderson, and R. Siddharthan (1993). On the characteristics of nonlinear soil response, *Bull. Seism. Soc. Am.* **83,** 218–244.

Zeghal, M., and A. W. Elgamal (1994). Analysis of site liquefaction using earthquake record, *Proc. Am. Soc. Civil Eng. J. Geotech. Eng. Div.* **120,** 996–1017.

Department of Earth Sciences
University of Southern California
Los Angeles, California, 90089-0740
(E.H.F.)

Southern California Earthquake Center
University of Southern California
Los Angeles, California, 90089-0740
(SCEC)

Manuscript received 12 September 2000.